

# An onshore-offshore interpretation of structures in the Devonian rocks of the Pentland Firth, Scotland using high resolution bathymetry and drone-enabled field observations.

Thomas A.G. Utley<sup>a,b</sup>, Robert E. Holdsworth<sup>b,c,\*</sup>, Richard J. Walker<sup>b</sup>, Edward D. Dempsey<sup>d</sup>, Ken J.W. McCaffrey<sup>b,c</sup>, Anna Dichiarante<sup>e</sup>, Thomas L. Jones<sup>b</sup>

<sup>a</sup> BP Exploration Operating Company Limited, Chertsey Road, Sunbury-on-Thames, Middlesex, TW16 7LN, UK

<sup>b</sup> Department of Earth Sciences, Durham University, Science Labs, Durham, DH1 3LE, UK

<sup>c</sup> Geospatial Research Ltd, Durham, UK

<sup>d</sup> School of Environmental Sciences, University of Hull, Hull, HU6 7RX, UK

<sup>e</sup> NORSTAR, Gunnar Randers Vei 15, N-2007, Kjeller, Norway

## ARTICLE INFO

### Keywords:

Bathymetry  
Faulting  
Folding  
Old Red Sandstone  
Devonian  
Orkney  
Caithness  
West of Shetland

## ABSTRACT

Strong tidal currents in the Pentland Firth separating NE Scotland and Orkney have stripped recent seafloor sediments revealing geological structures in parts of the Devonian Orcadian Basin that are otherwise limited to narrow coastal outcrops. Here we interpret and analyse a 220 km<sup>2</sup> high-resolution bathymetric dataset and combine these findings with onshore aerial imagery, field observations, and photogrammetric Virtual Outcrop Models created from coastal outcrops. This approach allows a reappraisal of the structure, stratigraphy and tectonic evolution of the Orcadian Basin, and gives new insights into fold and fault structures developed at sub-seismic to reservoir scales. A major basin-scale Devonian structure – the Brough-Brims-Risa Fault – can be traced from Caithness to Hoy and has partitioned reactivation-related deformation in the Orcadian Basin during later deformation episodes. Carboniferous inversion-related folds formed during E-W shortening are mapped and correlated between Caithness and Orkney. These structures are cross-cut by widespread highly connected fracture networks formed by steeply-dipping ENE-WSW and subordinate WNW-ESE trending structures developed during Permian NW-SE transtensional rifting. The offshore dataset demonstrates the continuity and topology of structures related to superimposed rifting and basin inversion events across a much greater scale range than was hitherto possible. [end].

## 1. Introduction

Recognizing the age and structural styles associated with individual deformation events in ancient basins, in addition to assessing the role of pre-existing structures, can be challenging and difficult to constrain (e.g. Tamas et al., 2022a). In offshore settings this may be due to the limited resolution, or absence of geophysical data (e.g. seismic reflection data), which can lead to significant uncertainties or contrasting models. Onshore areas may be limited by restricted or inaccessible surface exposures (e.g. steep coastal cliffs) and lack of evidence to constrain the absolute/relative age of fault movements. A better understanding of structural styles and reactivation histories can give key insights into basin development, fluid transport pathways, reservoir storage potential

and, more generally, to a reduction in sub-surface uncertainties. For example, Tamas et al. (2022a, 2023a, b) have recently shown how geochronological dating of syn-tectonic mineral fills associated with basin-related faults exposed onshore in the Inner Moray Firth Basin, Scotland, can be used to better constrain the age of correlative faulting episodes seen offshore. Similarly, in those parts of the same basin where datable syn-faulting mineralization is absent onshore, correlation of specific faults with those seen in offshore areas covered by good quality, well correlated seismic reflection data also allows the timing of movements to be better determined (e.g. Tamas et al., 2022b).

Recent studies by Collier et al. (2006), Nixon et al. (2012), Westhead et al. (2014), Sanderson et al. (2017), Yeomans et al. (2021), and Craven and Lloyd (2023) have used offshore bathymetric datasets around the

\* Corresponding author. Department of Earth Sciences, Durham University, Science Labs, Durham, DH1 3LE, UK.

E-mail address: [r.e.holdsworth@durham.ac.uk](mailto:r.e.holdsworth@durham.ac.uk) (R.E. Holdsworth).

<https://doi.org/10.1016/j.jsg.2023.104922>

Received 17 April 2023; Received in revised form 22 July 2023; Accepted 26 July 2023

Available online 29 July 2023

0191-8141/© 2023 The Authors. Published by Elsevier Ltd. This is an open access article under the CC BY license (<http://creativecommons.org/licenses/by/4.0/>).

UK to provide continuous images of the bedrock geology cropping out at the present seabed in areas lacking recent sediment cover. The seabed exposures can give a visually impressive new perspective on structural geometries and development. It provides a useful alternative to the use of seismic reflection data in offshore regions, especially in areas where such data are either absent, or are of low resolution. Furthermore, sea floor rock platforms are commonly developed in near-shore, shallow water settings where seismic data are difficult to capture whilst bathymetric data are generally of the highest quality. It is also a critical zone for the direct correlation of structures between onshore and offshore regions.

A 2 h difference in tidal phase on either side of the Pentland Firth drives tidal flow in the North Atlantic through this narrow channel into and out of the North Sea, generating currents with peak velocities of 5–6 ms<sup>-1</sup> (Draper et al., 2014 and references therein). These currents have scoured away recent sediment cover over a wide area of the seafloor. High resolution bathymetry was collected during feasibility studies for tidal power schemes, which spectacularly reveal the structure of the underlying bedrock.

In this paper, we use publicly available bathymetric data covering c. 220 km<sup>2</sup> (Figs. 1 and 2) to produce a new structural map of the offshore region separating mainland Scotland (Caithness) and the Orkney Islands. Analysis of these data provides new insights into the location and continuity of structures developed within the Devonian rocks of the Orcadian Basin, which are otherwise limited in exposure to narrow coastal outcrops. Field observations and desk studies have been supplemented using drone imagery and virtual outcrop models to further analyse the geology of inaccessible coastal exposures and correlate them

with the structures seen offshore. These rocks are commonly used as analogues to better understand the sedimentological and structural characteristics of Devonian sub-surface reservoirs offshore in the UK, most notably the Clair Field, the largest known hydrocarbon resource on the UKCS (Fig. 1a; Witt et al., 2010; Ogilvie et al., 2015; Robertson et al., 2020).

## 2. Regional setting

The Devonian Orcadian Basin occurs onshore and offshore in the Caithness, Orkney, and Moray Firth regions of northern Scotland, overlying Caledonian basement rocks of the Northern (Moine) and Central Highland or Grampian (Dalradian) terranes (Fig. 1a; Johnstone and Mykura 1989; Friend et al., 2000). It belongs to a regionally linked system of Devonian basins formed due to sinistral transtensional collapse of the Caledonian mountain belt that projects northwards into Shetland, western Norway and eastern Greenland (Seranne, 1992; Duncan and Buxton 1995; Woodcock and Strachan 2012). It is partially overlain by a number of Permian to Cenozoic, mainly offshore depocentres, including the West Orkney and Moray Firth basins (Fig. 1a).

Lower Devonian (Emsian) syn-rift alluvial fan and fluvial-lacustrine deposits are mostly restricted to the western fringes of the Moray Firth region (Rogers et al., 1989) and small areas of Caithness (NIREX, 1994a) and Orkney (Mykura et al., 1976a) occurring in a number of small fault-bounded basins of limited extent (Fig. 1b). These are overlain partially unconformably by Middle Devonian (Eifelian-Givetian) syn-rift alluvial, fluvial, lacustrine to locally marine and subordinate volcanic sequences that dominate the onshore sequences exposed in Caithness,

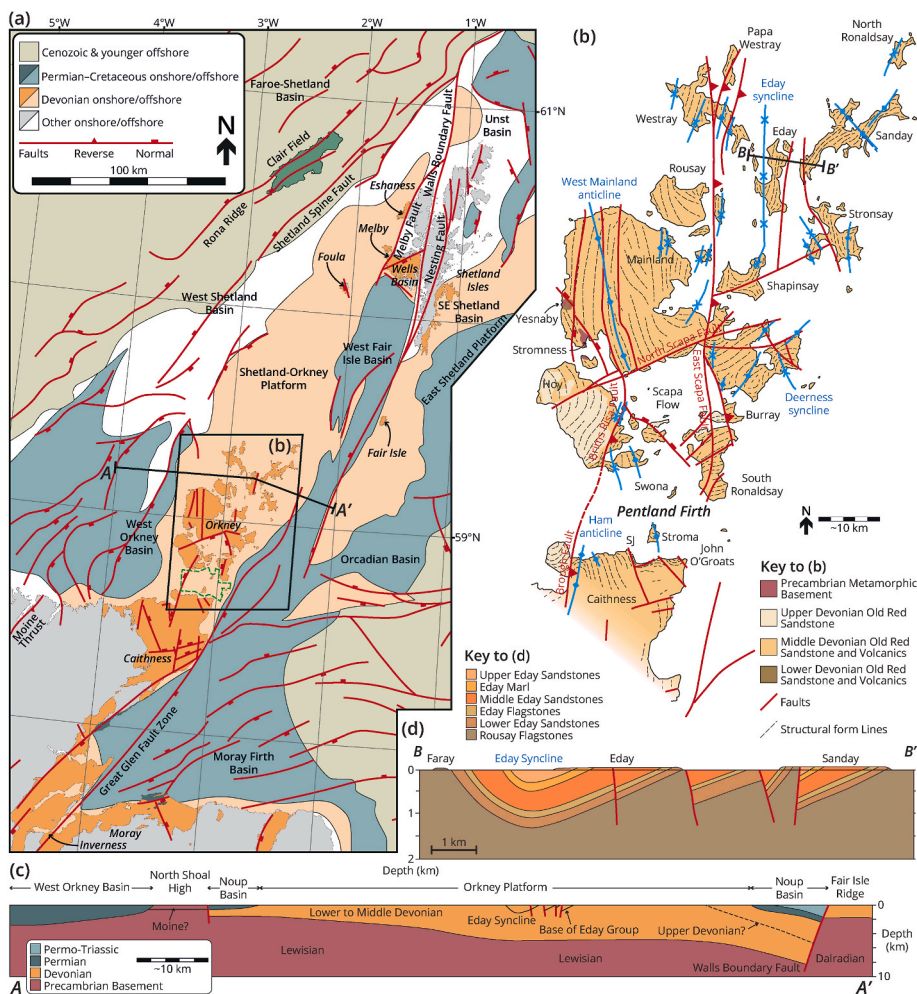
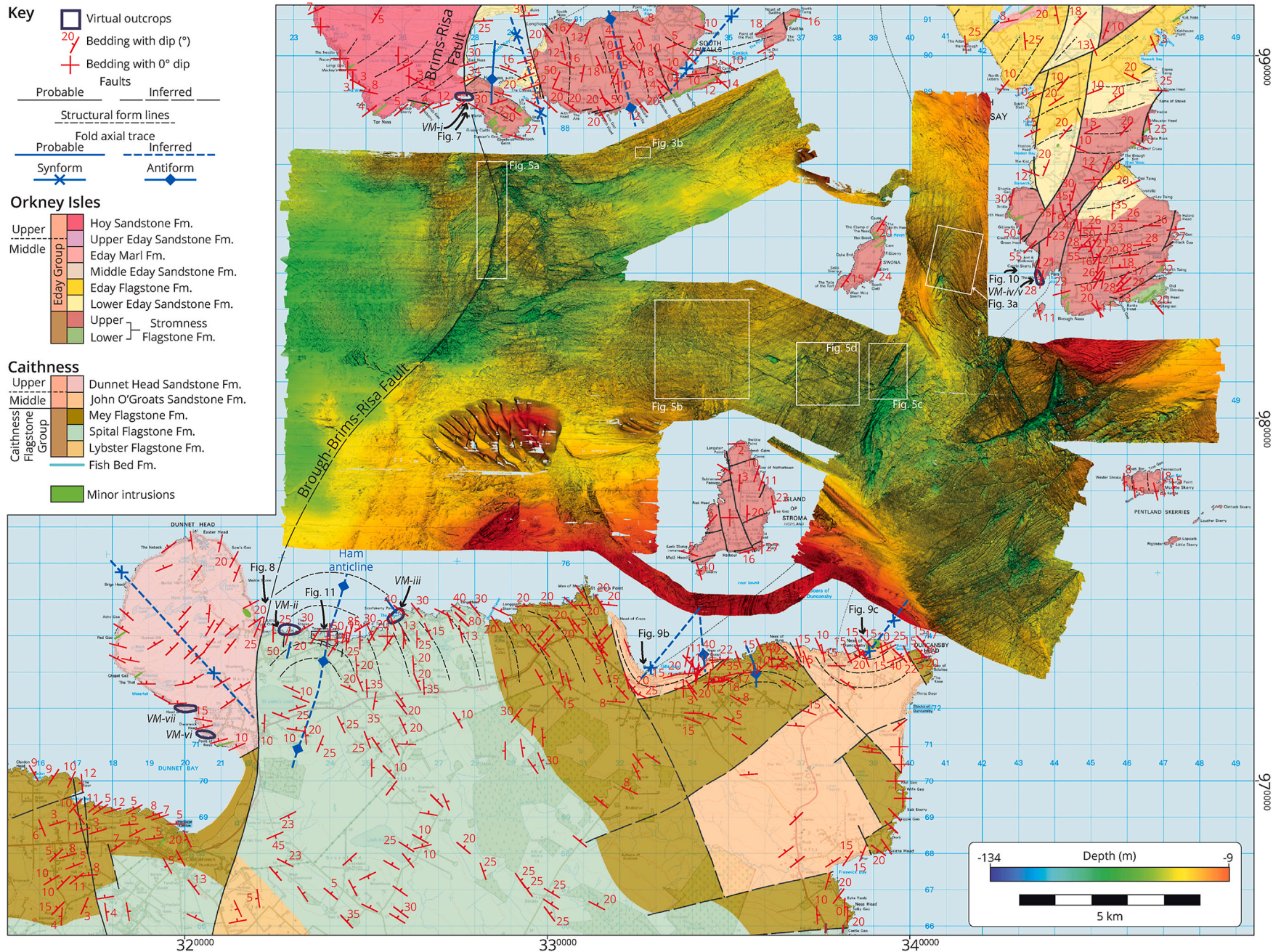


**Fig. 1.** (a) Regional map of the Orcadian Basin with Clair Oil Field highlighted. Modified after Dichiarante and Holdsworth (2016) and Oil and Gas Authority (2019). Green dashed box outlines location of Bathymetric survey. (b) Simplified geological map of Orkney and northeast Caithness with known principal structures shown. Modified after (Mykura et al., 1976a, b; BGS 1982, 1985a; Astin 1985, 1990; Brown et al., 2019). SJ = St John's Point. (c) Regional cross section through the Orkney-Shetland Platform showing the regional basement high which is flanked and overlain by Paleozoic sedimentary basins. Modified after (BGS 1985a). (d) Cross section through the Eday Syncline. Modified after (Mykura et al., 1976a, b; BGS 1982, 1985a). For location of cross section see Fig. 1b. (For interpretation of the references to colour in this figure legend, the reader is referred to the Web version of this article.)



Orkney and Shetland (Fig. 1a–c; Marshall and Hewett 2003). Upper Devonian (latest Givetian-Famennian), post-rift fluvial and marginal aeolian sedimentary rocks (Friend et al., 2000) are only found as fault-bounded outliers at Dunnet Head in Caithness, and the island of Hoy in Orkney (Fig. 1b).

Recent work (e.g. Wilson et al., 2010; Dichiarante, 2017; Dichiarante and Holdsworth, 2016; 2020a, b; Tamas et al., 2023a) has reappraised the structural evolution of the Devonian sedimentary sequences in onshore Caithness and Orkney. Three regional phases of outcrop-scale deformation have been recognised based on orientation, kinematics and associated fault rocks/vein fills.

- Group 1 faults are mainly N–S and NW–SE striking and record predominantly sinistral strike-slip to dip-slip extensional movements. They form the dominant outcrop-scale structures in the eastern regions closest to the offshore trace of the Great Glen Fault (GGF) (Fig. 1a). Basin-scale faults such as the Brough, Brims-Risa and North Scapa faults (Fig. 1b; Astin 1985, 1990; Hippler 1989, 1993; Dichiarante and Holdsworth, 2016; 2020a) are associated with significant sediment facies and thickness changes. Deformation bands, gouges and breccias associated with these faults display little or no associated mineralization or veining. Stress inversion analyses of fault and slickenline data suggests that these structures are related to Devonian ENE–WSW transtension associated with sinistral shear along the Great Glen Fault during formation of the Orcadian basin (Wilson et al., 2010; Dichiarante et al., 2020a).
- Group 2 structures are closely associated systems of metre-to kilometre-scale mainly N–S trending folds and thrusts related to a highly heterogeneous regional inversion event recognised locally throughout Caithness, Orkney and Shetland (Coward et al., 1989; Dichiarante et al., 2020a). Regional-scale structures include the shallowly plunging N/S trending open folds such as the Ham Anticline in Caithness and Eday Syncline in Orkney (Mykura et al., 1976a) (Fig. 1b–d). Once again, fault rocks associated with these structures display little or no associated mineralization or veining. Group 2 features are likely due to late Carboniferous to early Permian E–W shortening related to dextral reactivation of the Great Glen and Walls Boundary faults (Coward et al., 1989; Seranne, 1992; Dichiarante et al., 2020a; Armitage et al., 2020).
- Group 3 structures are the dominant features seen the Caithness coastal section west of St. John’s Point (SJ in Fig. 1b). They comprise dextral oblique NE–SW striking faults and sinistral ~ E–W to ENE–WSW striking faults with widespread syn-deformational low temperature hydrothermal carbonate mineralization ( $\pm$  base metal sulphides and bitumen, the latter sourced from local Devonian organic-rich strata) both along faults and in associated mineral veins (Dichiarante et al., 2016; 2020a, 2020b and references therein). Re–Os model ages of syn-deformational fault-hosted pyrite in Caithness yield Permian ages (ca. 267 Ma; Dichiarante et al., 2016). This is consistent with field observations that Group 3 fractures and mineralization are synchronous with the emplacement of ENE-trending lamprophyre dykes east of Thurso (intrusion ages of ca. 268–249 based on K–Ar dating; Baxter and Mitchell, 1984; Dichiarante et al., 2020a). Stress inversion of fault slickenline data associated with the carbonate-pyrite-bitumen mineralization imply NW–SE regional rifting (Dichiarante et al., 2016; 2020a), an episode also recognised farther west in the Caledonian basement of Sutherland (e.g. Wilson et al., 2010). There is no compelling evidence to suggest that structures with movements younger than the Permian are widespread or significant along the north coast section of Scotland (Dichiarante et al., 2016), although this cannot be completely ruled out.

### 3. Methods

Mapping of the seafloor geology and geomorphology of the Pentland Firth was carried out using bathymetric data (Fig. 2) (Survey: 2009 2011–147366 Isle of Stroma Pentland-Firth) sourced from the United Kingdom Hydrographic Office via the ADMIRALTY Marine Data Portal. Data coverage begins between 500 and 700m from the shoreline and covers an area of approximately 220 km<sup>2</sup> with large gaps (18–20 km<sup>2</sup>) in the data surrounding the islands of Swona and Stroma. Further details concerning the survey are given in Appendix A. The data were delivered in geoTIFF format (WGS, 1984 UTM 30N) with maximum vertical and horizontal resolutions of 6 mm and 2m respectively.

Bathymetric data were loaded into GlobalMapper v17.0 to produce hillshade, dip (slope) azimuth and slope angle maps (Fig. 3a–ii, iii, b–ii, iii, 4a–ii, iii), collection of orientation data (strike, dip, dip direction, Figs. 3 and 4) before export into ArcGIS 10.5 for mapping, geological interpretation and lineament analysis at 1:5000 scale. Having mapped out fault and fracture lineaments (Fig. 5), *fracture topology* - a network characterisation technique (Mauldon et al., 2001; Rohrbaugh et al., 2002; Sanderson and Nixon 2015) that simplifies a 2D fault or fracture network into discrete branches (fracture segments) and nodes (fracture connections) - was used to define both the geometrical features and network relationships between elements of the imaged fractures seen in the bathymetry (Fig. 6). This is a particularly useful way to describe fracture interconnectivity and therefore potential fluid transport properties. The proportions of the different types of nodes (I, T, X; Isolated tip – ‘I’, Terminating – ‘T’ – also known as ‘Y’ - and cross-cutting ‘X’), and the  $N_B/N_L$  ratio - number of fractures branches vs number of faults - can be used to determine the relative connectivity and spatial characteristics of the studied fracture network (Sanderson and Nixon 2015). The 2D topological analysis of bathymetry and aerial imagery was undertaken using the NetworkGT toolbox for ArcGIS (Nyberg et al., 2018). This was carried out to provide a quantitative assessment of fracture (lineament) connectivity using dimensionless intensity (2D fracture intensity  $\times$  average branch length), a scale invariant measure of fracture intensity which takes into account sampling bias (Sanderson and Nixon 2015; Nyberg et al., 2018). To investigate the spatial variability in the fracture patterns further, a series of 2.8 km<sup>2</sup> square sample boxes ( $n = 14$ ) were used to sub-sample the nodal and fracture trace length map (Fig. 6a). Box size was chosen to maximise the number of fractures sampled. Sample positions were chosen to investigate differences in fracture intensity and connectivity adjacent to the major faults (e.g. the Brough-Brims-Risa fault and the sinistral strike slip fault north of Duncansby Head) and across the km-scale N–S trending folds present in the offshore region (Figs 2, 4av).

Fieldwork was carried out in both Orkney and Caithness to ground-truth interpretations and investigate the outcrop-scale expression of structures observed in bathymetric data in coastal sections adjacent to the offshore study area. The use of an aerial drone allowed images to be collected from several inaccessible cliff sections that were used to create 3D Structure from Motion (SfM) Virtual Outcrop Models. Models were generated in Agisoft Photoscan and were analysed and interpreted within the VRGS software package (Hodgetts 2019) to extract geological orientation data. Links to a selection of these models are presented in Appendix B (VMI–vii) of the Supplementary Materials and their locations are shown on Fig. 2. Structural analysis was carried out using Stereonet 9.5 and the study was supplemented using high resolution aerial imagery courtesy of the Ordnance Survey via Digimap and published onshore and offshore geological maps (and bedding orientation data) (BGS 1982, 1985a, 1985b, 1986, 1999, 2019). A fracture topology analysis was also carried out in one particularly large and well exposed rock platform within the hinge region of the regional scale Ham anticline (Fig. 2). The approach used followed that used offshore, with the spatial variability in the fracture patterns being further investigated using square sample boxes to sub-sample the nodal and fracture trace length map. This allowed a comparison of onshore and offshore topology

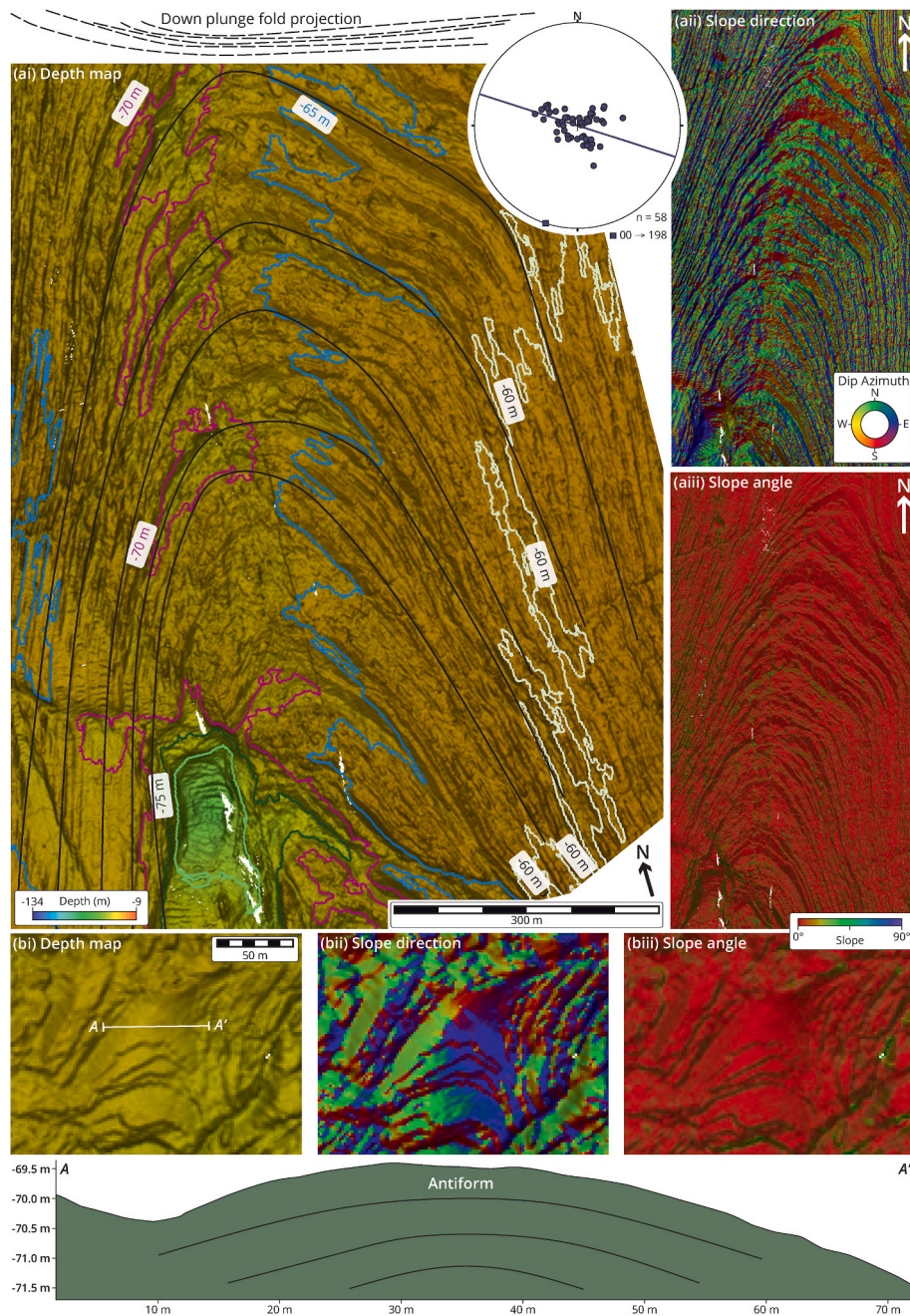


**Fig. 3.** Detailed bathymetric images of examples of fold structures in the Pentland Firth. (a) Major gently S-plunging km-scale synform between South Ronaldsay and Swona with down plunge projection showing fold geometry; stereonet shown poles to bedding and interpreted profile plane and beta axis (regional fold plunge). (b) smaller Dm-scale northerly plunging anticline offshore South Walls, with down-plunge projection. For locations, see Fig. 2.

datasets, albeit at different scales.

#### 4. Geology and submarine geomorphology of the Pentland Firth

##### 4.1. Seabed morphology

Water depths in the Pentland Firth range up to 135m, with the seabed dominated by rocky sea floor and exposed swept bedrock, classified as “Atlantic and Mediterranean high energy infralittoral rock” (EUNSIS, 2007-11 Scheme) (Shields et al., 2009; Martin-Short et al., 2015). These areas of swept bedrock reveal the underlying geological structure of the Devonian rocks in the Pentland Firth, accentuated by the differential erosion of weaker geological structures (e.g. fault and fracture zones) and stratigraphic units (e.g. shales and siltstones) (Figs. 2–6).

Many faults and associated damage zones have been eroded to depths many tens of metres below that of the surrounding sea floor, forming distinct gullies and chasms that can extend for many kilometres along strike (Figs. 2 and 5).

Local areas of modern marine sediment are preserved, such as the 10–20m high SE-NW longitudinal dunes and the 4 × 3 km dune field rising to a height of 15 m located respectively E and W of Stroma (Fig. 2; for further details and analysis, see Appendix A). Bottom sampling shows that the unconsolidated sediments are predominantly composed of poorly-to well-sorted coarse sands, fine gravels and gravel-sized, benthic bioclasts (BGS 2019).

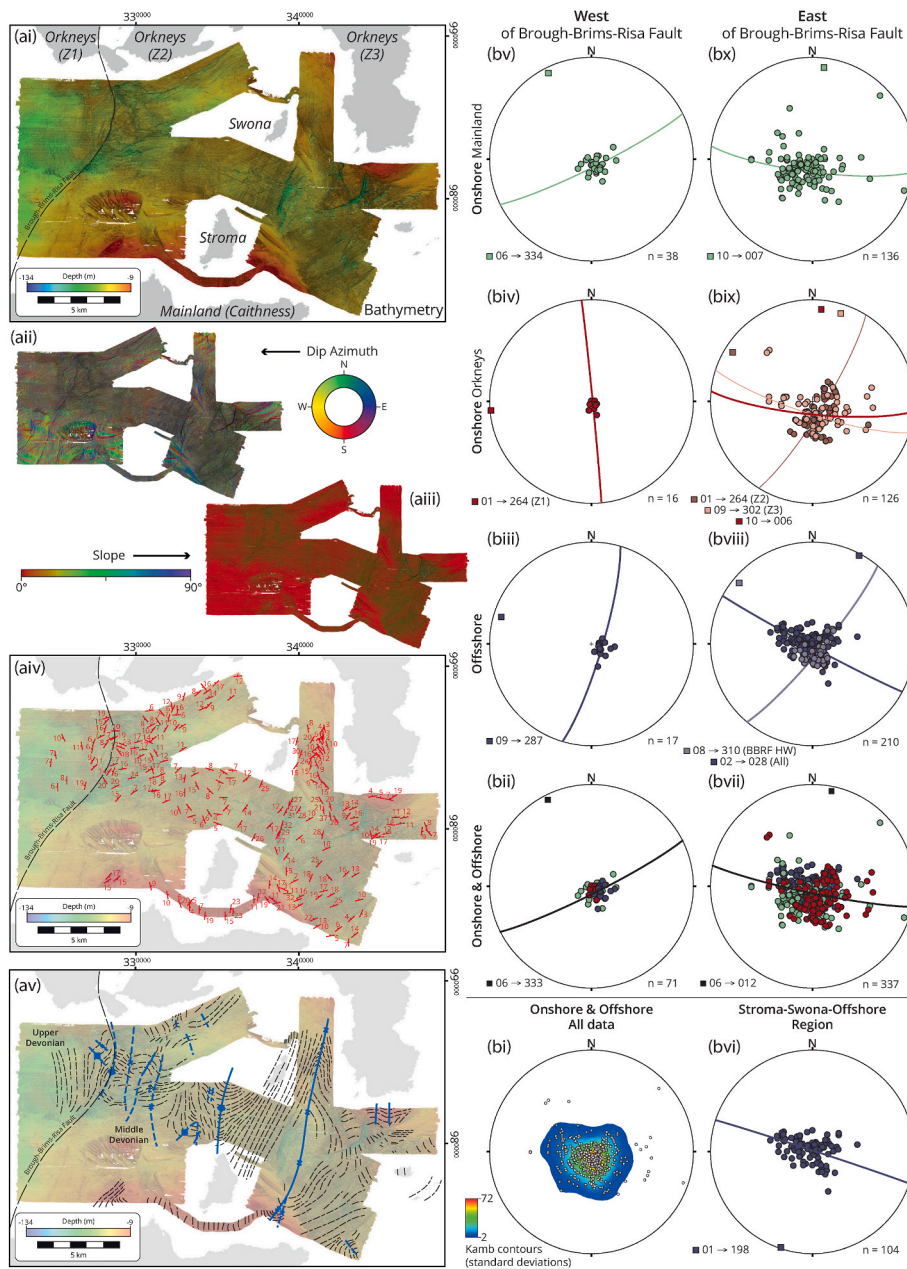


**Fig. 4.** (a) Form map highlighting the offshore Pentland Firth, showing (ai) uninterpreted bathymetry, (aii) derived dip azimuth and (aiii) slope, (aiv) extracted bedding dips, and (av) form lines and major fold structures. (b) Equal area stereoplots showing poles to bedding for (bottom to top) (i) the entire study area; (ii-v, left column) the onshore-offshore regions west of the BBRFZ; and (vi-x, right column) the onshore-offshore regions east of the BBRFZ. Interpreted profile planes and beta axes are shown. Colour coding is used to indicate specific datasets as indicated. (For interpretation of the references to colour in this figure legend, the reader is referred to the Web version of this article.)

#### 4.2. Stratigraphy

Onshore outcrops in Caithness are dominated by Middle Devonian sedimentary rocks of the Caithness Flagstone Group (Fig. 2), which is subdivided into the Lybster Flagstone, Spital Flagstone and Mey Flagstone formations (BGS 1985b, 1986). These formations are predominantly fluvial and lacustrine in origin and contain several fossil-rich horizons or ‘fish beds’ (Johnstone and Mykura 1989), most notably the Achanarras Fish Bed Member that separates the Lybster and Spital Flagstone formations. They are overlain by the predominantly fluvial sedimentary rocks of the John O’Groats Sandstone Group. Upper Devonian fluvial and aeolian sedimentary rocks of the Dunnet Head Sandstone Group are restricted to the headland of Dunnet Head (see virtual outcrop models Vi and VII, Appendix B) and are faulted against older rocks to the east by the Brough Fault (Fig. 2) (Johnstone and Mykura 1989; Dichiarante et al., 2020a).

On Orkney, Middle to Upper Devonian sedimentary rocks and minor volcanics dominate and are the lateral equivalents to the Caithness

Flagstone Group (Fig. 2; Mykura et al., 1976a). The lacustrine Upper and Lower Stromness Flagstone formations – separated by the Sandwick Fish Bed Member (BGS 1999) – are overlain by the rocks of the Eday Group, which preserve a transition from mixed lacustrine and marginal fluvial/alluvial deposits to predominantly fluvial deposits. The Upper Devonian Hoy Sandstone on the island of Hoy is formed by a ~1 km thick sequence of fluvial and aeolian sandstones and marls that unconformably overlie lavas and tuffs of the Middle Devonian Eday Group known as the Hoy Volcanics (Mykura et al., 1976a; BGS 1999). They are a faulted against other parts of the Eday Group by the Brims-Risa Fault which has long been correlated on regional geological grounds with the Brough Fault in Caithness (Fig. 1b and 2) (Coward et al., 1989; Mykura et al., 1976a; Seranne, 1992).

Based on their likely continuity with adjacent onshore outcrops, it seems likely that the seafloor west of the Brough-Brims-Risa Fault in the offshore survey area (see below) comprises Upper Devonian units equivalent to those seen onshore in Hoy (Fig. 2). To the east of the fault, it is likely that the sea floor comprises Middle Devonian units from the

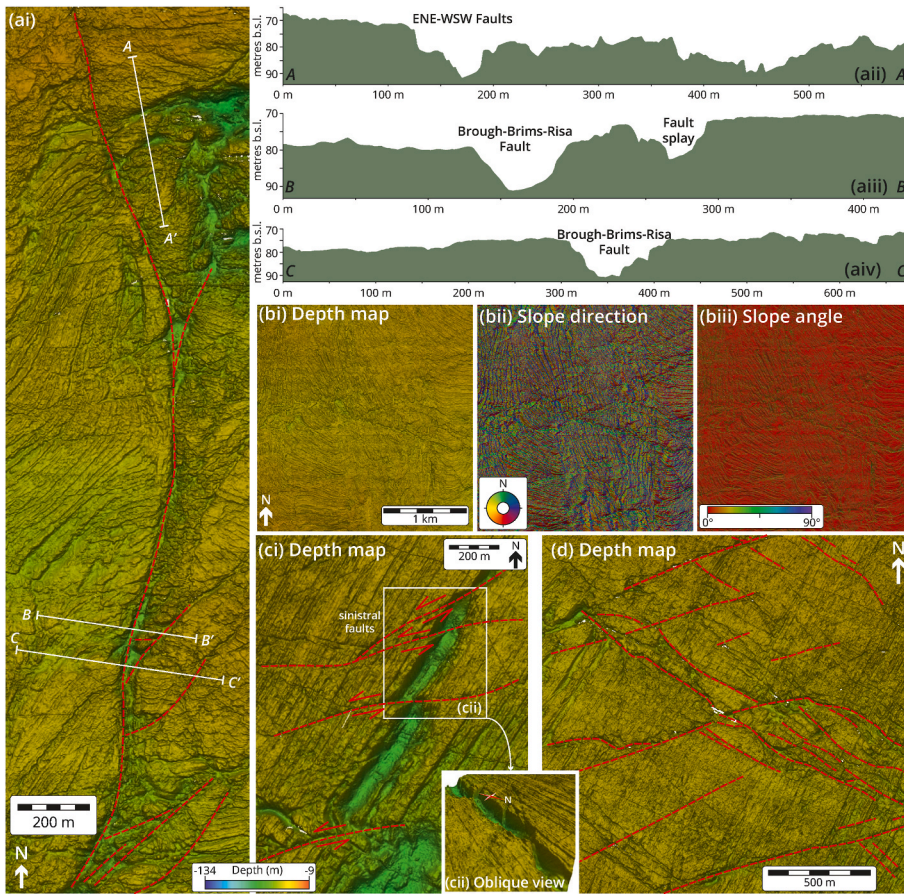


**Fig. 5.** Detailed images of examples of faults and fracture systems in the Pentland Firth – for locations see Fig. 2. (a) i-iv Maps and cross sections of the deeply eroded BBRFZ offshore and subordinate fault zones. (b) Faulting associated with more diverse fold patterns and highly variable bedding orientations east of the BBRFZ. (c) Apparent sinistral offsets of submarine bedding planes. Inset shows oblique view. (d) Rectilinear pattern of lineaments in the area between Stroma and Swona. Dip azimuth and slope colours are as in Figs. 3 and 4. (For interpretation of the references to colour in this figure legend, the reader is referred to the Web version of this article.)

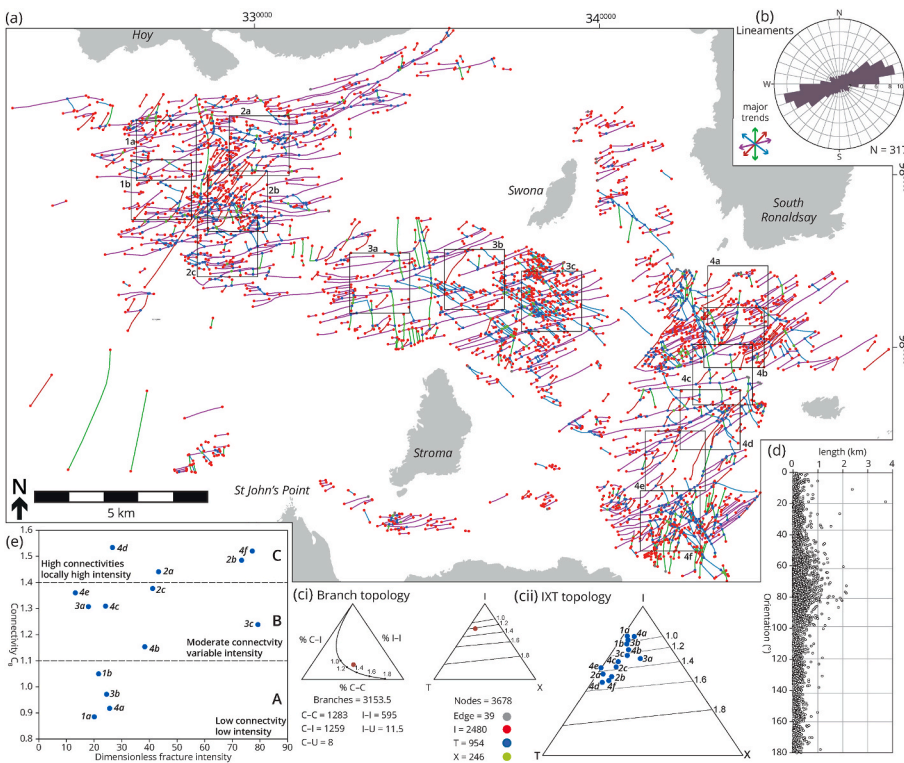


**Fig. 6.** (a) Topological analysis of mapped lineaments. Orientation of lineaments subdivided by set and nodes coloured by node type. Boxes show location of sampled sub-areas presented in Fig. 6c and e. (b) Length weighted rose diagram of mapped lineaments showing 4 major trends; N-S, ENE-WSW, NE-SW and NW-SE. (c) Ternary diagrams showing branch and node topology for mapped lineaments. (d) Length vs orientation plot for mapped lineaments. (e) Plot of fracture intensity vs Connectivity ( $C_B$ ) for the various sub-areas shown in Fig. 6a. Heat maps of Nodal Density are also shown in Appendix C, Figure C1.

Caithness-Stromness Flagstones and overlying units. A more detailed stratigraphic assignment has not been attempted and may be challenging, although it may be possible in the future to attempt to differentiate and contrast units that are more sand-rich and massive (e.g. aeolian/fluvial deposits), from those that are more heterogeneously layered, and likely represent more interbedded/stratified units (e.g. lacustrine deposits).

#### 4.3. Offshore structural geology

Various styles of faulting and folding are observed in the offshore study area, and it is mostly possible to link larger (km-scale) structures mapped onshore with those exposed on the seafloor, providing an almost continuous structural map of the Pentland Firth and surrounding area (Figs. 2, 4a and 6a). Bedding was distinguished from fracture and fault lineaments based partially on the dip of the adjacent sea floor, but also from the morphology of the lineament, which is best seen in oblique section views. Faults tend to form straight, deeply eroded lineaments, as opposed to regularly spaced and often more asymmetric lineaments created by dip and scarp surfaces across bedding (e.g. Figs. 3 and 5). The kinematics of faults are inferred from the apparent offset of bedding traces where visible (pixel resolution ~2 m), but vertical throws are difficult to assess. Further constraints come from known senses of offset and displacement for faults with particular trends seen in the adjacent onshore areas (e.g. BGS 1985a, b, 1986, 1999, 2019; Dichiarante 2017; Dichiarante and Holdsworth, 2016, 2020a, b).

The sinuous trace of the generally NNE-SSW Brough-Brims-Risa Fault Zone (BBRFZ, Figs. 2 and 4a, b, 5a, 6a) divides the region into two distinct domains. The strata immediately to the west of the fault appear to be less deformed, with bedding gently dipping towards the W and NW (Fig. 4a, bi-v) together with a lower number, density and diversity of fault lineaments. An importance caveat here is that the region to the west of the BBRFZ trace is less well exposed over a smaller area of seafloor. Nevertheless, the apparently less deformed state is consistent with these rocks being Upper Devonian strata, as onshore (at Dunnet Head and Hoy) they are typically less affected by deformation compared to the Middle Devonian strata (Dichiarante 2017). The region to the east of the BBRFZ is generally more folded (e.g. Figs. 2 and 4a) with more variable bedding orientations (Fig. 4bi, vi-x) and a higher concentration of fault and fracture lineaments (Fig. 6a). This variation is due in part to the presence of several km-scale N-S oriented fold structures (Figs 2, 4avi, v) in addition to the development of localised zones of complexity and folding related to major fault zones.

**Folds:** The bathymetry reveals the presence of several large, km-scale, upright to shallowly plunging, open to gentle fold structures trending generally NNE-SSW to NW-SE (Figs. 2–4). A large N-S trending, N-closing fold can be traced for ~18 km along strike running from the west coast of South Ronaldsay down to the region offshore and to the north of John O'Groats (Figs. 2 and 4a). A down plunge projection cross section of this fold reveals a slightly asymmetrical open syncline which plunges extremely shallowly towards the south (Fig. 3ai-iv) with gentle (120–180°) interlimb angles, and a slight eastward vergence. The highly oblique cut through this structure on the seafloor makes the fold appear tighter than it actually is, a common feature in offshore bathymetric surveys through folded strata (e.g. Craven and Lloyd 2023). Another smaller (dm-to hm-scale) northward-plunging and -closing open anticline (interlimb angle approximately 150°) is exposed on the seafloor 1 km south of South Walls (Figs 2, 3bi-iv). Bedding orientation data from the offshore region east of the BBRFZ (Fig.4bviii) reveal an almost subhorizontal NNE-SSW regional fold plunge, whilst those in the central offshore area between the islands of Stroma and Swona plunge very shallowly to the SSW (Fig. 4bv).

To the west of the large synform, a N-S trending anticline is observed, with the hinge running southwards towards the island of Stroma which seems to represent the southward continuation of this very gentle fold hinge zone (Figs. 2 and 4a). A series of less well-defined

N-S folds are seen in the region west of this anticline and may link northwards into folds of similar trend seen onshore in South Walls and easternmost Hoy in the region east of the BBRFZ (Fig. 4a); the northward continuation of the Ham Anticline on Caithness is not exposed and may be cut out by the BBRFZ northwards.

A series of very open (Interlimb angle (ILA) > 150°), NW-SE folds are seen in the region immediately to the west of the BBRFZ, south of Hoy (Figs. 2 and 4a, bii-v). A gentle synclinal fold with the same NW-SE trend is also seen in the Upper Devonian rocks at Dunnet Head in Caithness, west of the Brough Fault (Fig. 2; 4a, bv). Furthermore, bedding data from onshore Hoy, west of the BBRFZ reveal very open, shallowly W-plunging folds (Fig. 4biv). Subordinate NW-SE folding is also seen in the onshore data from Orkney in the region immediately to the east of the BBRFZ (Fig. 4bix) and at Dunnet Head onshore in Caithness (Fig. 4bv, x).

**Faults and fractures:** A total of 3178 offshore lineaments interpreted to be related to brittle fractures (no discernible offset observed) and faults (where offset could be observed) were mapped from the bathymetry (Fig. 5a-f, 6a), with a cumulative trace length of >1500 km, a mean length of 247.96 m and a maximum of 3717.55 m (Table 1). Four trends are identified, with ENE-WSW (n = 1607) being the predominant set, in addition to NE-SW (n = 443), WNW-ESE to NW-SE (n = 740), and N-S (n = 388) (Fig. 6a and b). The longest lineaments are orientated N-S to NE-SW, and ENE-WSW (Fig. 6d).

The correlation of the Brough and Brims Risa faults in Caithness and Orkney, respectively, has long been accepted based on the association with Upper Devonian strata to the west of the fault traces and similarly complex movement histories (e.g. Mykura et al., 1976a, 1976b; Coward et al., 1989); the sea-floor lineaments also clearly line up in the bathymetry (Fig. 2). The BBRFZ forms the longest mapped lineament, with several segments up to 3–4 km long, and trending NNW-SSE to NE-SW

**Table 1**

Comparison of fracture data from the onshore and offshore Pentland Firth.

Sample Area	Onshore	Offshore
Area (m <sup>2</sup> )	60889.22	1005053316.79
No. Lineaments	8077	3178
Mean Lineament Length (m)	3.05	247.96
Max Lineament Length (m)	45.13	3717.55
StDev Lineament Length (m)	3.53	257.28
Mean Lineament Orientation (°)	82.49	74.16
StDev Lineament Orientation (°)	42.48	46.12
No. Edge Nodes (E)	215.00	39.00
No. I Nodes (I)	2358.00	2479.00
No. X Nodes (X)	669.00	246.00
No. Y Nodes (Y)	3623.00	953.00
No. Unknown Nodes (U)	0.00	0.00
No. Nodes	6650.00	3678.00
No. Branches	7951.50	3161.00
No. Lines	2990.50	1716.00
No. Connections	4292.00	1199.00
Average Connect/Line	2.87	1.40
Average Line Length (m)	8.21	1010.25
Average Branch Length (m)	3.09	607.06
Average Connect/Branch	1.70	1.22
2D Intensity	0.40313	0.00174
Dimensionless Intensity	1.24449	0.83033
No. Branches (minus unknown branches)	7939.50	3153.50
No. C - C (doubly connected branches)	5737.00	1281.00
No. C - I (singly connected branches)	1864.00	1258.00
No. C - U (singly connected branches)	92.50	8.00
No. I - I (isolated branches)	234.00	595.00
No. I - U (singly connected branches)	12.00	11.50
No. U - U (unknown/edge branches)	0.00	0.00
Total Length C - C (m)	15517.42	513847.72
Total Length C - I (m)	6442.53	626695.92
Total Length C - U (m)	1118.40	10792.43
Total Length I - I (m)	1200.65	348663.71
Total Length I - U (m)	200.16	7070.10
Total Length U - U (m)	67.40	0.00
Total Trace Length (m)	24546.57	1507069.88

with a total exposed length of ~12 km (Figs. 2, 5ai and 6a). This structure typically is associated with a 10–15 m deep gully feature with several NNE to NE trending splays developed on its eastern flank (Fig. 5ai-iv). These structures are concentrated in the area where the fault swings from a NE to NNW trend and may have formed due to strain localisation adjacent to a restraining and/or releasing bend during oblique movement on, or reactivation of, the fault. In the immediate area surrounding the fault zone, particularly in the hanging wall, bedding is difficult to identify, probably corresponding to a damage zone up to 200 m wide, with numerous subordinate faults and smaller folds (Figs. 2, 4a and 5ai, 6a). Other prominent N–S lineaments (NNW to NNE) up to ~1 km long are found in the region north of Stroma and running through the region between South Ronaldsay and John O’Groats (Figs 2, 5bi-iii, 6a).

Regionally, the most numerous, laterally extensive and deeply eroded lineament set trends ENE–WSW (Fig. 5b–d, 6a, b, d). Many of these features show apparent sinistral offsets, particularly where they bisect and offset the trend of dipping beds (e.g. Fig. 5c and d). A subordinate set of WNW–ESE to NW–SE trending lineaments appear to form an apparent conjugate set to the ENE–WSW trending lineaments and show some apparent dextral offsets (Fig. 5d). These structures are generally some of the shortest in length and commonly terminate against ENE–WSW and NE–SW trending lineaments. Both ENE–WSW and NW–SE sets appear to cross-cut the larger fold structures in the region. Swarms of these fault/fracture sets produce a pronounced rectilinear pattern, particularly in the area between Stroma and Swona (Figs. 2, 5d and 6a).

**Fault and fracture topology:** Topological analysis for the entire offshore region shows a low level of connectivity with I nodes dominant

(Fig. 6a, c). Fracture branches with C–C (doubly connected) topology are dominant, although the presence of a significant number of C–I and I–I branches means that the  $C_B$  (number of connections per fracture branch) value of approximately 1.2 confirms the low overall connectivity (Fig. 6c). A high number of I nodes and the low proportion of X nodes suggest that many fractures do not crosscut and remain isolated.

As a result of the apparent spatial clustering displayed by the NE–SW to N–S and the ENE–WSW fracture sets, the intensity of fracturing varies across the sample area of exposed bedrock (Fig. 6a). Our sample boxes were chosen to investigate differences in fracture intensity and connectivity adjacent to the major faults and across the km-scale N–S trending folds present in the offshore region (Figs. 2, 4 and 5). Across the 14 sample areas, dimensionless fracture intensity values vary between 13.3 and 79 and the connections per branch ( $C_B$ ) varies from low (0.9–1.1) to moderate (>1.4) values (Fig. 6e). Areas of high to moderate connectivity correspond to the hangingwall region of the BBRFZ (Samples 2a–c) and the region to the north of the Duncansby Head which lie close to the ENE–WSW sinistral strike slip fault and its immediate side-walls (Samples 4c–f) (see also maps in Appendix C, Fig. C1). All other samples areas displayed moderate or low connectivity ( $C_B < 1.1$ ). High fracture intensity does not always correspond to higher connectivity (Fig. 6e).

#### 4.4. Onshore structural geology

**Brough-Brims-Risa Fault Zone (BBRFZ):** On the south coast of Hoy, the Brims-Risa fault juxtaposes Upper Devonian rocks of the Hoy Sandstone Formation against the Middle Devonian Upper Stromness Flagstone and Lower Eday Sandstone formations (Fig. 2). The Brims-Risa

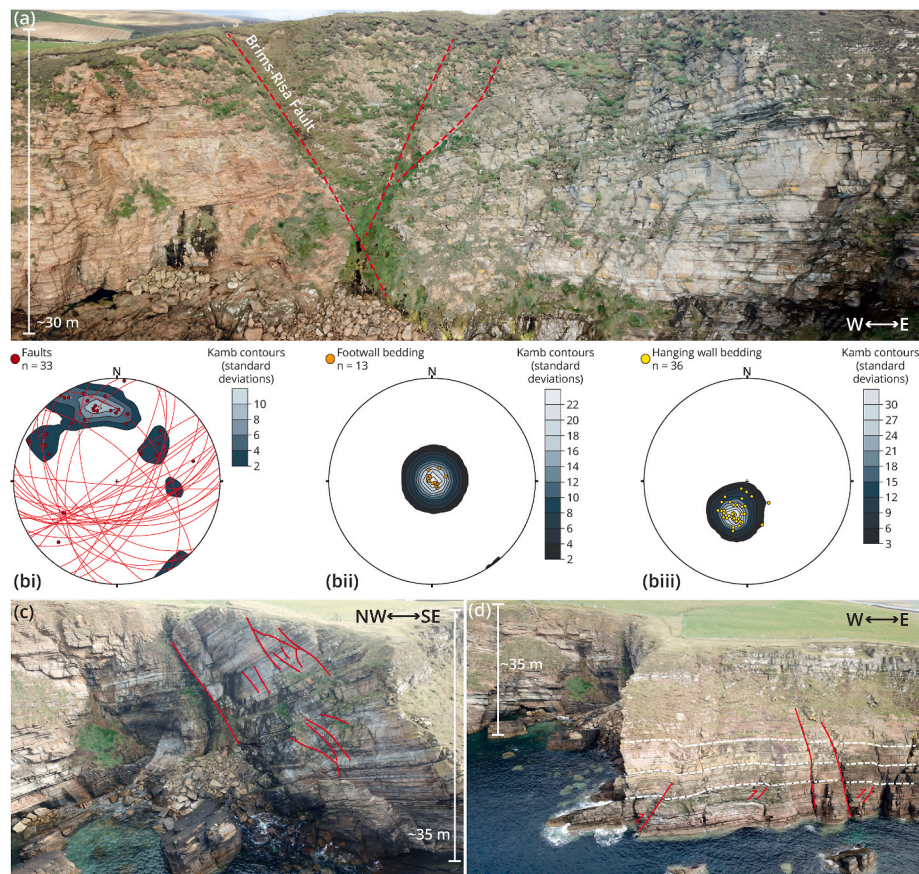


**Fig. 7.** Onshore exposure of the Brims Risa Fault Zone at The Witter, Hoy [ND 327783 988866] (a) Drone image of the Brims Fault in cliffs near The Witter. (b) Stereonets of structural data derived from 3D photogrammetric model of the coastline at The Witter, Hoy (See VMI, Appendix B, Supplementary Material). (c) Drone image of ENE/WSW trending fault zones. (d) Drone image of folding and faulting in the hanging wall of the Brims-Risa fault.

Fault is exposed but inaccessible near The Witter [ND 327783 988866] where the fault dips  $\sim 50^\circ$  towards the NE (150/50NE, in the convention strike, dip, dip direction) (Fig. 7a; see also virtual outcrop VMi, Appendix B). The thin-bedded flaggy sandstones of the Upper Stromness Flagstone that lie in the hangingwall of the fault are faulted against more thickly bedded red-orange sandstones of the Upper Devonian Hoy Sandstone Formation in the footwall. The apparently reverse offset here is consistent with the suggestion that the Brims-Risa fault is a Group 1 Devonian-age normal fault strongly inverted during late Carboniferous (Group 2) E-W shortening (Coward et al., 1989; Dichiarante et al., 2020a). This is also consistent with the observation that bedding in the fault footwall is generally very shallowly dipping (Fig. 7bii) containing few faults, whilst the Middle Devonian strata in the hangingwall dip moderately NE (Fig. 7biii) and are fractured and faulted throughout (Fig. 7bi, c). The dominant fault trends (Fig. 7bi) are ENE-WSW, NE-SW and NNE-SSW with normal to oblique slip senses. Inland, at the Witter Quarry [ND 327945 989146], north-dipping flagstones are cut by similarly oriented NE-SW trending normal faults and NE-SW to EW trending subvertical extension fractures, which are partially mineralized with calcite.

On the north coast of Caithness, the N-S-trending Brough Fault passes through the harbour north of the village of Brough [ND 322097 973978] (Fig. 2). Here, Upper Devonian rocks of the Dunnet Head Sandstone Group to the west are juxtaposed against the Middle Devonian Spital Flagstone Formation to the east (Fig. 8a–c). The fault core runs through the harbour, though not exposed, forming a marked gully feature in the cliff and foreshore (Fig. 8a, c).

In the cliffs to the east of the fault trace, bedding dips are generally shallow to moderate W-dipping with small-scale westerly verging NNE-SSW Group 2 folds plunging gently SSW (Fig. 8b). Several much larger Group 2 folds are exposed in the cliffs along the coast for several hundred metres to the east of the Brough Fault and one fold pair, at Langyop [ND 322880 974189] (see also virtual outcrop VMii, Appendix B), is accessible on foot. Here a shallowly north-plunging, westerly-verging open fold pair is exposed (Fig. 8d), which is cut by two ENE-dipping thrust faults (Fig. 8e). Axial planes trend N-S to NNE-SSW and dip steeply E. All these folds are consistent with Group 2 inversion due to E-W shortening along the Brough Fault. As shown by Dichiarante et al. (2020a), these folds are everywhere cross-cut by moderately to steeply dipping dextral oblique normal to dextral strike slip faults trending N-S to NE-SW. These faults are widely associated with calcite mineralization in veins and local breccias and a stress inversion analysis of faults exhibiting slickenlines gives a NW-SE extension direction consistent with Group 3 structures regionally.

The exposures of Upper Devonian strata lying immediately to the west of the Brough Fault are strongly deformed (Fig. 8c). Bedding in the small islands known as The Clett and in the wave cut platform to the west is generally steeply dipping to sub-vertical and strikes sub-parallel to the Brough Fault. In The Clett, the bedding dips steeply to the E and is overturned (Enfield 1988), whilst strata exposed in the foreshore to the west are steeply dipping, but young eastwards based on cross-bedding in the sandstones (Fig. 8c; Dichiarante et al., 2020a). This suggests that a tight synclinal fold lies in the unexposed region that separates The Clett from the remainder of the foreshore to the west (Fig. 8c). Traced further west into the cliffs on the north side of Dunnet Head, the bedding dips become much shallower. Thus, the steepening of bedding close to the fault is thought to reflect deformation related to movements along the Brough Fault (Trewin 1993). A series of moderately to steeply plunging, metre to tens of metre-scale, open to tight N-S trending Z folds are exposed in the sub-vertical strata of the foreshore area and also appear to deform a small Permian volcanic vent (Fig. 8c; Dichiarante et al., 2020a). This deformation is interpreted to be the result of Permian (Group 3) dextral shear along the immediately adjacent Brough Fault. Since the closure direction of the unexposed syncline cannot be determined, it is impossible to say whether this is an older Group 2 fold formed during E-W shortening, or a Group 3 structure formed due to

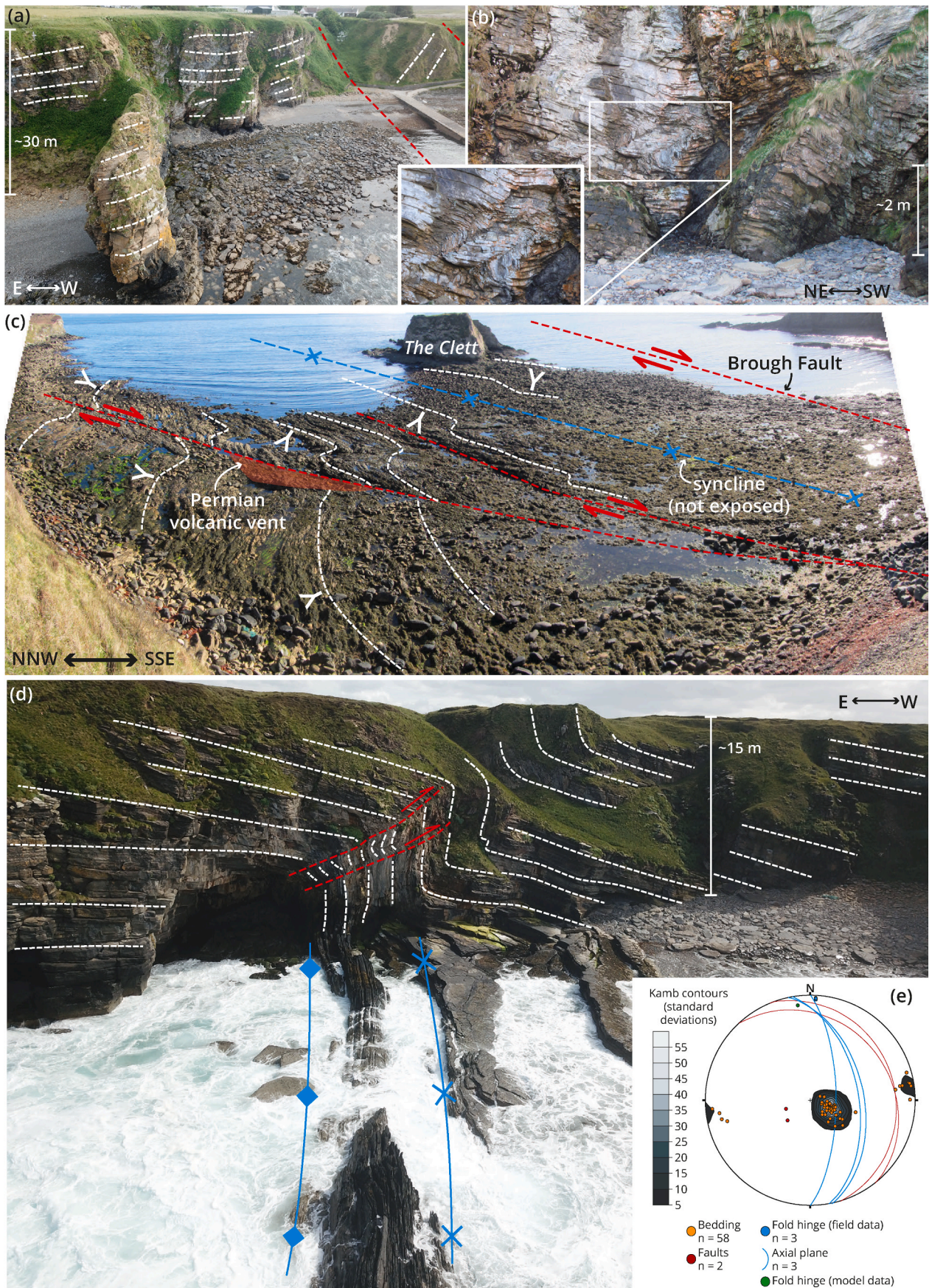
later dextral reactivation of the Brough Fault.

**Faults and folds:** In Caithness and Orkney, the Ham Anticline and Eday Syncline (Fig. 1b), respectively, are the principal regionally recognised folds. These folds are generally accepted as being related to Group 2 deformation associated with regional inversion during the Carboniferous (Mykura et al., 1976a; Coward et al., 1989; Dichiarante 2017; Dichiarante et al., 2020a). They are N-S trending, low amplitude, gently plunging, long wavelength structures. Smaller scale N-S folds form cm-to dm-scale localized fault-related structures, through to large, km-scale folds are also recognised all across Caithness and Orkney (e.g. Figs. 2 and 4a, bi, vii, ix, x, 7–10; Enfield and Coward 1987; Coward et al., 1989; Dichiarante 2017; Dichiarante et al., 2020a) and are most widely developed east of the BBRFZ.

A series of regional scale N-plunging folds (Figs. 2 and 9a) are recognised along the N coast from Brough Harbour towards Duncansby Head, some of which can be traced offshore using the bathymetry. In Gills Bay [ND 332848 972824] rocks of the John O'Groats Sandstone Formation are folded into an open NE-trending, gently plunging syncline (Fig. 9bi-ii). Near Ness of Duncansby, strata from the same unit are folded into another open NE trending, gently N plunging syncline (Fig. 9ci-ii). Close to the hinge of this fold, an undeformed small, volcanic vent outcrops which comprises monchiquites and tuffs (Chapman 1975). Macintyre et al. (1981) obtained a poorly defined K–Ar age of c. 270 Ma from these intrusive units suggesting that they are related to a series of regionally recognised Permian volcanic vents and minor intrusions in Caithness-Orkney (Fig. 2). A poorly exposed anticline runs out through the coast at the Ness of Quoys and is apparently offset by a large ENE-WSW fault lying immediately to the south with an inferred sinistral-normal shear sense (Figs. 2, 9a and 12). The folds are separated by three, mostly poorly exposed NW-SE faults in the region between St John's Point and Duncansby Head (Fig. 9a). One of these faults outcrops as a steeply SW-dipping structure exposed in the cliffs near to Thirle Door, on the southeast side of Duncansby Head (Trewin, 1993). Here, the apparently normal displacement and absence of mineralization associated with faulting has led Dichiarante (2017) to conclude that these NW-SE faults are Group 1 (i.e. Devonian) normal faults.

Other small-scale NW-SE trending folds have been recognised by Dichiarante et al. (2020a) in onshore Caithness in two structural settings. The first, exemplified by the metre-scale WNW-ESE-oriented folds exposed at St John's Point (location shown on Fig. 1b), are interpreted to have formed due to Group 3 sinistral shear along closely associated sets of ENE-WSW bounding faults (Dichiarante et al., 2020a, their Fig. 12). The second set are more complex and are associated with NW-SE fault zones as seen at Skarfskerry (Fig. 2; see also virtual outcrop VMiii, Appendix B). Here, unusually tight NNW-SSE to NW-SE folds are preserved adjacent to a fault zone characterized by the intense development of early Neptunian dykes and other soft-sediment deformation structures in the immediate wall rocks. This has been interpreted by Dichiarante et al. (2020a) to represent a Group 1 fault active at the time of deposition of the Devonian strata that was then obliquely inverted by sinistral transpression during Group 2 E-W shortening. Most of these structures are likely below the resolution of the offshore bathymetry and are much tighter than the NW-SE folds recognised offshore.

As in Caithness, numerous smaller (cm-dm) scale Group 2 folds, and associated thrust structures are exposed along the coastal sections in Orkney (Dichiarante 2017). For example, along the southwestern most part of South Ronaldsay, several N- to NE-trending fault zones are well exposed in rather inaccessible cliff sections (Fig. 10). In Horse Geo [ND 343140 984995] (see also virtual outcrop VMiv, Appendix B) for example, a deeply eroded gully corresponding to an ENE-WSW trending Group 3 fault zone exposes an array of N-S orientated, ramp and flat thrusts, back thrusts, fault propagation folds and reactivated normal faults (Fig. 10a). Further to the north at Tainga [ND 342703 986012], (Fig. 10b) closely spaced (0.5–1m) top-to-the-west thrusts and folds locally steepen the bedding with small, distributed reverse offsets. To the south at The Wing [ND 343599 983915] (see also virtual outcrop



(caption on next page)

**Fig. 8.** (a) Oblique aerial overview image of Brough Harbour showing the onshore exposure of the Brough Fault in Brough Harbour, Caithness [ND 322105 974007]. Main fault passes close to the position of the jetty (b) Oblique field photograph of Group 2 folding and reverse faulting in the Middle Devonian rocks in the eastern hanging wall of the Brough Fault. *Inset* detailed image of W-verging folds. (c) Oblique view looking ENE of Group 3 folds and faulting in the Upper Devonian strata exposed in The Clett and foreshore region which lie in the immediate western footwall of the Brough Fault. The location of the deformed volcanic vent described by Dichiarante et al. (2020a) is also shown. (d) Drone image of intense W-verging Group 2 folding and localised deformation in the Spital Flagstone Formation at Langypo [ND 322880 974189]. (e) Stereonet of structural data collected in the field, supplemented by data derived from 3D photogrammetric model (see VMii, Appendix B, Supplementary Material).

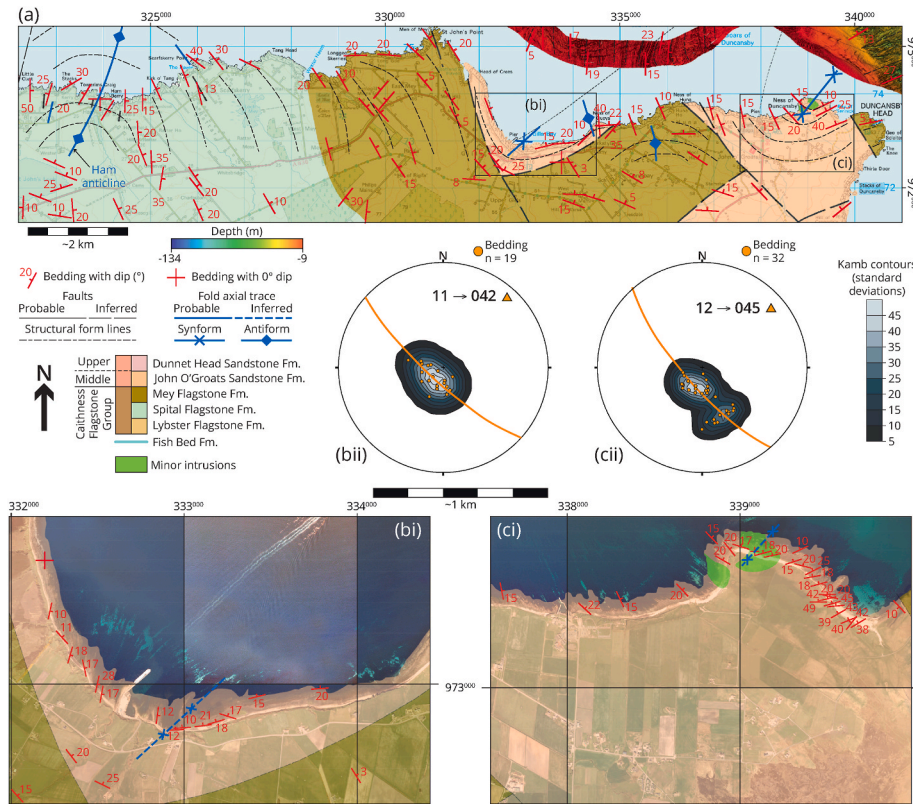


**Fig. 9.** Mapping of regional scale fold structures around the southern margin of the Pentland Firth. (a) Geological map of coastline from Brough to John O'Groats showing long wavelength fold structures, faults and bedding. (b) i) Aerial image and ii) stereonet of syncline at Gills Bay. (c) i) Aerial image and ii) stereonet of syncline at Ness of Duncansby. Bedding data sourced from the BGS and supplemented with additional field data. Stereonets show profile plane and plunge/trend of fold (beta) axis. Lower hemisphere equal area projections. Aerial images courtesy of the Ordnance Survey.

VMv, Appendix B) a large E-dipping fold and thrust zone (Fig. 10 c-e) is exposed which appears to be truncated westwards against a N-S orientated steeply dipping fault zone (red plane shown in Fig. 10c) which seems to act as a local buttress.

**Onshore fracture networks and topology:** A topological analysis of fracture networks was carried out using an orthorectified aerial image of the coastline, west of Ham Harbour, where fractures cutting part of the hinge region of the Ham Anticline are exceptionally well exposed [ND 323912 973928]. A total of 8077 lineaments were mapped from the aerial imagery with a trace length of ~24.5 km, a mean length of 3.05 m and maximum of 45.13 m (Table 1 and Fig. 11a). Mapped lineaments correspond to faults and fractures, with three principal trends identified: ENE-WSW to E-W ( $n = 3216$ ); NNE-SSW to N-S ( $n = 3417$ ); and NW-SE ( $n = 1444$ ) (Fig. 11b).

ENE-WSW to E-W trending lineaments are the most numerous and spatially extensive across the rock platform and form discrete corridors of fractures (Fig. 11a). The longest lineaments correspond to the three dominant trends that are observed (Fig. 11c). Topological analysis shows a moderate level of connectivity (overall  $C_B$  of ca. 1.7), with Y nodes dominant (Fig. 11d). Branch topology shows a high degree of connectivity with C-C (doubly connected) branches being the most numerous (Fig. 11d). A high number of Y nodes and low proportion of X nodes suggest that many fractures do not crosscut or remain isolated. The three sample boxes (HA1-3) display variable fracture intensity values (from 4.5 to 27.5) and all show relatively high values of connectivity ( $C_B$  1.7–1.8) (Fig. 11e) compared to the offshore datasets. The

highest connectivity values were recorded in the centre of the rock platform where all of the major fracture sets are present, including one long N-S fracture that provides connectivity to other clusters in the sample area (see also maps in Appendix C, Fig. C2). Due to coastal erosion, other N-S orientated faults zones and associated structures are under-represented here, with connectivity in these areas likely being higher.

## 5. Discussion

### 5.1. Onshore-offshore correlation and fold patterns

A fully interpreted geological and structural map of the onshore-offshore region surrounding the Pentland Firth is shown in Fig. 12. The folds and faults mapped using bathymetry from the Pentland Firth show that the regional-scale structures and trends seen in both Orkney and Caithness (e.g. Fig. 1b) are broadly continuous and consistent. Structures representing all three phases of deformation seen onshore (Groups 1–3 of Dichiarante et al., 2020a) can be identified offshore with varying degrees of confidence.

Group 1 structures are the most difficult to recognise as they are commonly obscured by later deformation and reactivation, as is the case onshore (Dichiarante et al., 2020a). Such structures likely include the BBRFZ, and many of the other NW to N, and sometimes NE trending faults such as those that lie offshore of South Ronaldsay (Fig. 12).

Group 2 fold structures are more easily recognised and include the

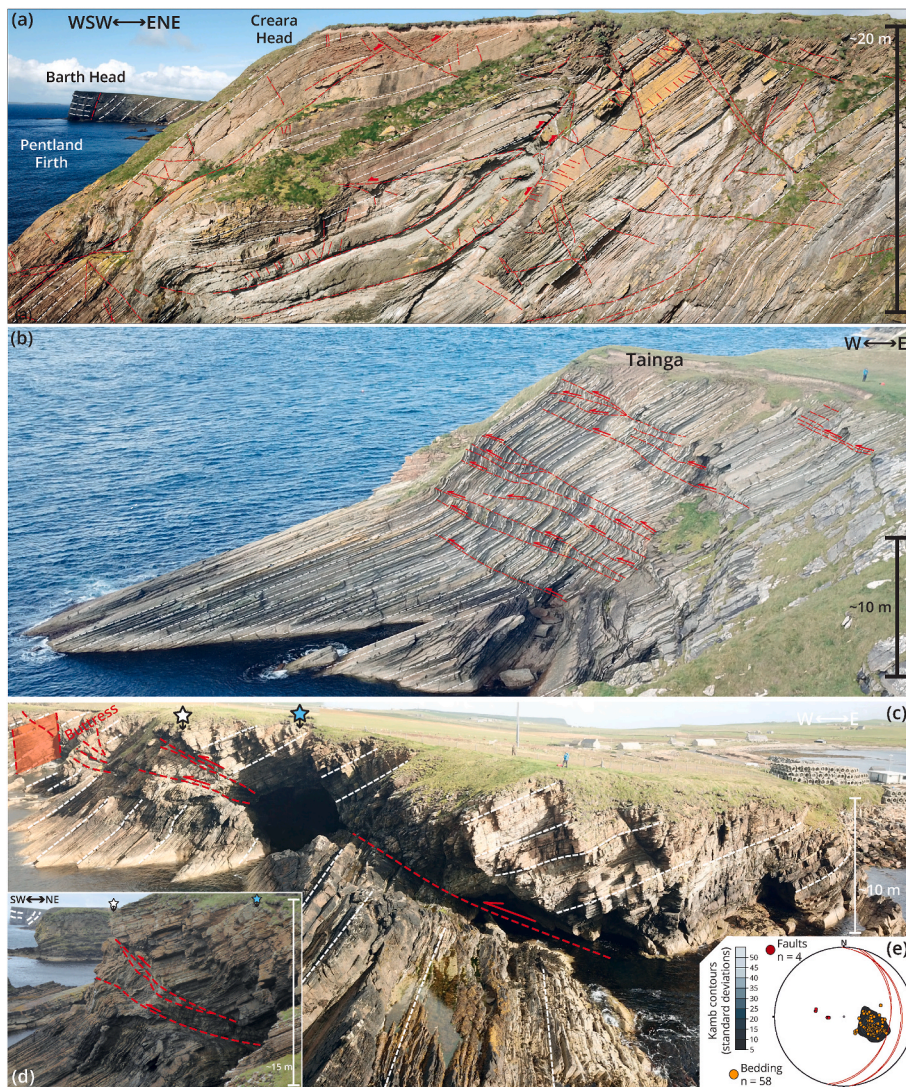


**Fig. 10.** Drone images of complex polyphase structures related to repeated oblique reactivation that are developed along the coastline of South Ronaldsay, Orkney. (a) Polyphase deformation exposed in the cliffs on the Northern side of Horse Geo [ND 343140 984995], an eroded ENE-trending fault zone (see also VMiv, Appendix B, Supplementary Material). The headland of Barth Head [ND 342655 985574] can be seen in the background which is cut by a significant North/South trending steeply dipping sub-vertical fault, which may be the onshore continuation of a deeply eroded lineament observed on bathymetric data immediately to the south. (b) Distributed Group 2 fault propagation folds and thrusts exposed at Tainga, South Ronaldsay, Orkney Isles [ND 342703 986012]. (c) Aerial image of Group 2 thrust fault exposed at The Wing, near Burwick, South Ronaldsay, Orkney Isles [ND 343599 983915]. (d) Detail of fault zone showing distorted and contorted bedding in a zone bound by two top-to-the-west thrusts. (e) Stereonet of structural data derived from 3D photogrammetric model (see also VMv, Appendix B, Supplementary Material).

widespread N-S- to NNE-SSW-trending folds that have been mapped both onshore and offshore. Many of the smaller scale and locally complex low angle or bedding-parallel thrust and fold structures seen onshore which are locally prominent in coastal cliff sections (e.g. Figs. 7, 8d and 10) are difficult to identify on the bathymetry and are probably mostly below the resolution of the data.

Group 3 structures likely include reactivated N-S faults such as the BBRFZ, as well as sinistral ENE-WSW and more localised dextral NW-SE trending structures associated with regional transtension during the Permian (Dichiarante and Holdsworth, 2016; 2020a). Onshore, some of the ENE-WSW trending structures correspond to the traces of faults and/or Permian age dykes, such as those mapped onshore at Castletown (Dichiarante et al., 2020a). It seems likely that similar intrusions also occur offshore, but distinguishing such features from fault lineaments has, so far, not proved possible. NW-SE faults with dextral Group 3 displacements are also recognised onshore, most notably at Skarfskerry where dextral Reidel shears and cm-scale steeply plunging Z folds are exposed overprinting all other structures in the reactivated Group 1 fault core exposed in the harbour (Dichiarante et al., 2020a; their Fig. 10f). This suggests that the subordinate NW-SE dextral faults seen offshore may correspond to reactivated Group 1 faults.

In the relatively limited area of exposed rock lying to the west of the BBRFZ, deformation appears to be less intense, both onshore and offshore, with fewer large-scale folds like those observed in the hanging

wall (Fig. 12). Dichiarante et al. (2020a) followed Coward et al. (1989) by proposing that the Brough-Brims-Risa fault initiated as an E-side-down basin-, or sub-basin-controlling Group 1 normal fault during the Devonian. The development of N-S to NNE-SSW trending, E- and W-verging Group 2 folds both onshore and offshore east of the BBRFZ in most of the study area (Figs. 2, 4a and 9a) is consistent with E-W compression and inversion in Permo-Carboniferous times. The relative lack of Group 2 deformation structures west of the BBRFZ suggests that this fault system acted as a buttress, preventing deformation from propagating further to the west. This is also consistent with proposed links between dextral reactivation of the Great Glen Fault and E-W compression and inversion (Coward et al., 1989; Wilson et al., 2010; Seranne 1992).

There is good onshore evidence for Group 3 reactivation of the Brough Fault as a dextral strike-slip Group 3 structure during the Permian (e.g. Fig. 8c; Dichiarante et al., 2020a). The open NW-SE trending folds seen offshore and onshore (Dunnet Head, Hoy) in the Upper Devonian strata exposed west of the Brough-Brims Risa fault (Figs. 2 and 4a, bii-v, viii, ix, 12) are most likely transtension-related structures like those seen on a smaller scale at a number of onshore locations adjacent to reactivated N-S to NE-SW-trending Group 1 faults (e.g. Bridge of Forrass fault, Dichiarante et al., 2020a).

The ~1–2 km gap between the regions covered by the bathymetry and the onshore exposures makes it difficult to unequivocally link all

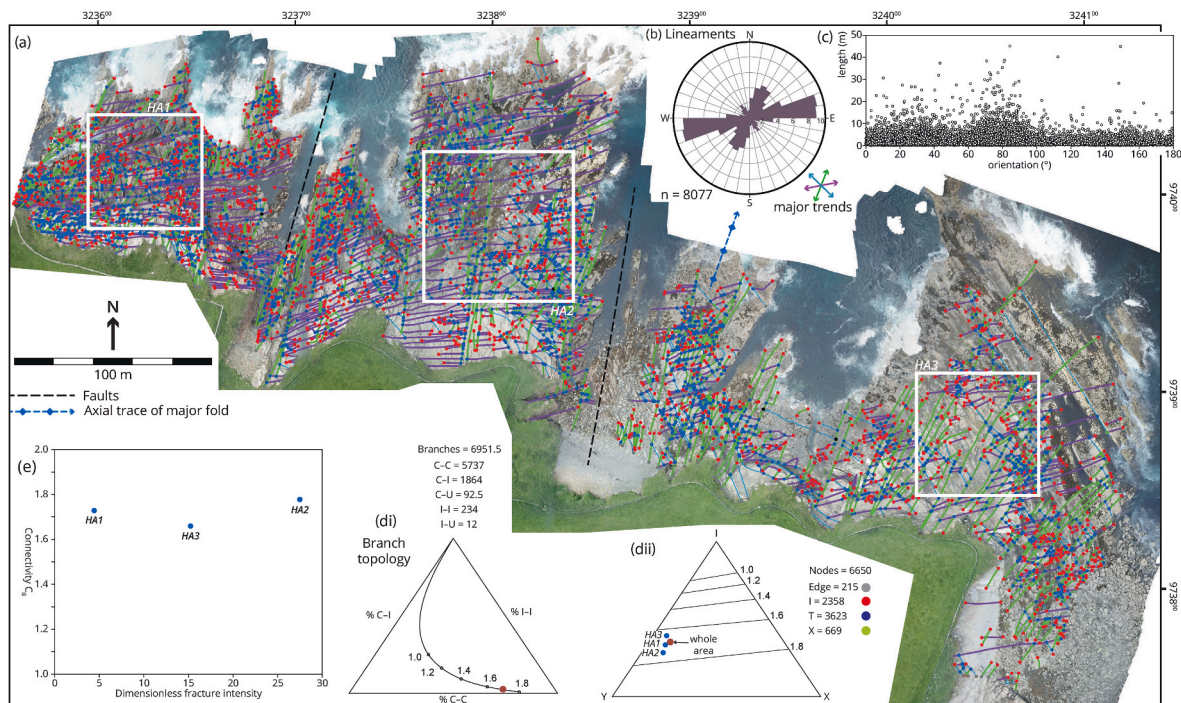


**Fig. 11.** (a) Orthorectified aerial image of fracturing in the hinge region of the Ham Anticline with interpreted lineaments with three principal trends identified; ENE-WSW, N-S to NE-SW and NW-SE. (b) Length weighted rose diagram of mapped lineaments. (c) Plot of lineament length vs orientation. (d) Ternary diagrams showing branch and node topology. (e) Plot of fracture intensity vs Connectivity ( $C_B$ ) for the various sub-areas shown in Fig. 11a. Heat maps of Nodal Density are also shown in Appendix C, Figure C2.

faults and folds recognised in the two domains, a common problem that is encountered in onshore-offshore studies of this kind (e.g. Craven and Lloyd 2023). Nevertheless, it is possible to make some broad connections between major folds mapped in onshore regions, to those seen offshore. The prominent N-S syncline running between South Ronaldsay and Swona appears to represent the northward continuation of the open syncline exposed in Caithness at the Ness of Duncansby (Figs. 2, 9a and 12). This fold, and the antiform that lies to the west of it appear to be offset by a prominent apparently sinistral ENE-WSW fault that passes through the Caithness coastline just east of the Ness of Quoys. The poorly exposed anticline and well exposed syncline located still further to the west around Gills Bay, appear to merge into a fold pair imaged in the bathymetry south of the island of Stroma. The island itself is dominated onshore by flat-lying strata cut by prominent N-S faults that plausibly correspond to the hinge zone of the major open antiform seen in the bathymetry immediately to the north of the island (Figs. 2, 4a and 12).

Offshore from Hoy and South Walls, a series of N-S folds seen onshore seem to correspond to a series of folds offshore with similar trends in the region located to the east of the Brims-Risa Fault (Figs. 2, 4a and 12). A large gap in the exposed bedrock further to the south means that it is unclear whether some of these folds are broadly equivalent to the Ham Anticline and associated folds in Caithness, although this seems likely (i.e. they are all Group 2 structures).

One other notable feature of the folds is that those onshore in Orkney and Caithness appear to be generally plunging gently to the north (e.g. Fig. 4bix, x) whilst those in the central part of the offshore region are subhorizontal (Fig. 4bviii), or plunge shallowly S (Fig. 4bvi). Confirmation of this change comes from the closed elongate basin shape of the syncline that runs between South Ronaldsay and the Ness of Duncansby (Figs. 2, 4a and 12). This kilometre-scale change in fold plunge implies the presence of a regional-scale plunge depression beneath that Pentland Firth. It is possible that this bedrock structure may have exerted an influence over the location of the much younger Quaternary seaway.

## 5.2. Fracture patterns and resource implications

The bathymetric data used in this study could be considered to be roughly equivalent in terms of spatial coverage and resolution to a Z (horizontal) slice from a 3D seismic volume. The fault zones in the Orcadian Basin show various levels of complexity across a range of scales, with much of that observed complexity, at or below the resolution of the bathymetry and by proxy would likely also not be seismically resolvable.

If the Orcadian Basin is viewed as a potential analogue to fractured reservoirs offshore, it appears that brittle deformation is concentrated around major N-S trending structures such as the BBRFZ and the ENE-WSW strike-slip fault north of Duncansby Head (Fig. 6a, e, 12) and longer N-S fractures in the onshore regions (Fig. 11). However, these N-S structures do not in general affect a large volume of rock and, as shown by the topology study, it is only locally adjacent to these structures that higher connectivity occurs. On a larger scale, our analysis shows that areas such as the footwall to the BBRFZ and the central part of the Pentland Firth with km-scale open fold structures have lower fracture intensity and low connectivity. In contrast, areas in the hangingwall to the BBRFZ and sidewalls of the ENE-WSW strike-slip fault north of Duncansby Head show higher connectivity, but variable fracture intensities. Higher connectivity requires all of the N-S to NE-SW, NW-SE, ENE-WSW and WNW-ESE structures to co-exist, but in particular, it seems to be the presence or absence of the apparently most clustered fracture set, the N-S fractures, that affects the connectivity onshore and offshore by connecting the other systems. From this we infer that in a reservoir appraisal study, it would be important to not only characterise the major seismic-scale structures, but also the geometrical and spatial properties of the smaller-scale fractures that are more widely distributed and of different orientations to the major structures. Using our example as an analogue, the presence of major seismic-scale faults and at least two further distributed sub-seismic-scale fracture sets would be required to provide the fracture connectivity to effectively deliver fluids to or from a wellbore.

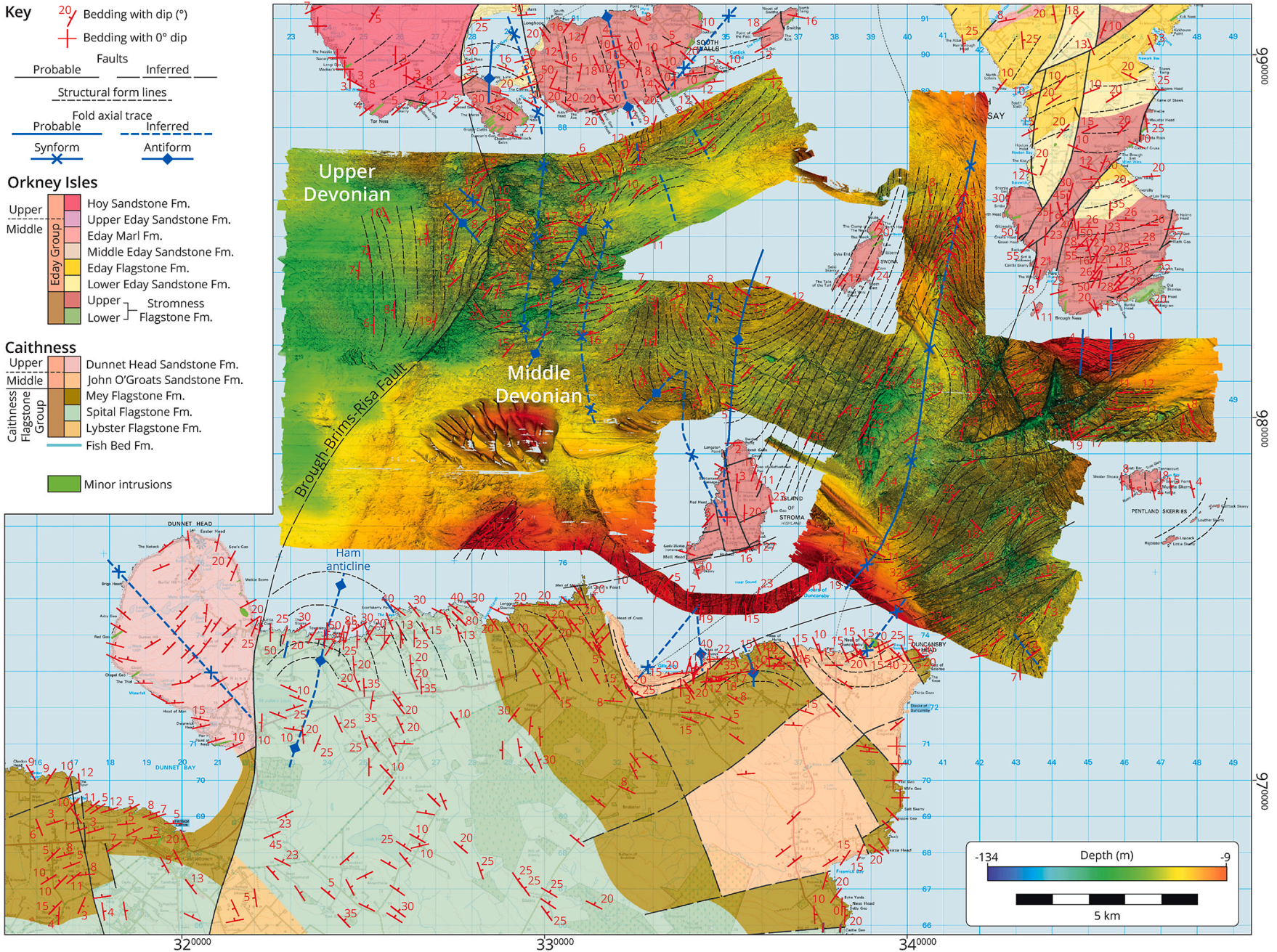


Fig. 12. Summary interpretation of the onshore and offshore geological structure of the Pentland Firth.

The km-scale fold structures identified in this study may be analogous to trapping structures, in geometry and size, to those that host hydrocarbons seen in offshore data elsewhere. Offshore, many of Devonian sequences in the northern part of the UKCS are buried beneath significant thicknesses of Mesozoic and Cenozoic fine grained lithologies and Zechstein evaporites. These younger sequences prevent detailed imaging of the deeper structures which underlie potential seals to hydrocarbon accumulations sourced from Devonian and Carboniferous source rocks. Thus, the Pentland Firth structures give a potential insight into the nature, scales and geometries of structures in these deeper underexplored Palaeozoic plays (see also Tamas *et al.* 2022).

## 6. Conclusions

Recently acquired offshore multibeam bathymetry in combination with aerial imagery, photogrammetric 3D virtual outcrop models and fieldwork to ground truth observations, provides new insights into the size, shape, continuity, distribution and complexity of the structures within the Orcadian Basin across a range of scales. Analysis of a 220 km<sup>2</sup> survey of the Pentland Firth has produced a new structural map of the offshore region (Fig. 12) and reveals aspects of the structure and geology of the region that are sometimes poorly exposed or inaccessible onshore. The findings further re-enforce the observation that structural complexity in surface/seabed outcrops at all scales in the Orcadian Basin reflect both local reactivation of pre-existing faults during regional inversion events and superimposition of obliquely-orientated rifting episodes during later basin development (e.g. Dichiarante *et al.*, 2020a, b, Tamas *et al.* 2021; 2023a, b).

The dominant structure is a 12 km long roughly N/S trending curvilinear lineament which is interpreted as the offshore continuation of the BBRFZ, likely as one linked structure. This key basin-wide structure seems to partition later deformation and inversion acting as a buttress to reactivation, with well-developed N–S-trending, long (km scale) wavelength folds and complex fault/fold relationships well developed mainly to the east of the structure. These almost certainly correspond to Group 2 structures of Late Carboniferous age linked to E–W shortening and inversion related to dextral reactivation of the Great Glen Fault. The rocks adjacent to the BBRFZ both onshore and offshore also preserve evidence for later dextral transtensional reactivation during Group 3, NW–SE Permian rifting. A series of mostly gentle NW–SE trending folds formed during transtensional deformation are recognised, particularly – but not exclusively – in the otherwise less deformed Upper Devonian strata in the footwall of the BBRFZ.

Numerous faults and fractures have been mapped offshore and fracture topology analysis has identified 4 predominant trends; ENE–WSW, NE–SW, WNW–ESE to NW–SE and N–S, which are consistent with trends identified during previous studies onshore and offshore. Major N–S fault zones are connected to a wider rock mass by later crosscutting and connecting fracture systems. Fault and fracture networks appear to be better connected at higher resolutions. These findings may have implications for hydrocarbon exploration and development, and future operations in the under explored and more poorly understood Palaeozoic basins of the Moray Firth, East Shetland Platform, East Orkney Basin, and many areas associated with the Faroe Shetland Basin west of Shetland, including the Clair Basin.

Finally, multidisciplinary onshore-offshore studies such as this will likely become more commonplace for offshore wind, tidal power and marine geohazard projects where a detailed description of the seafloor geomorphology is integrated with geological interpretation as part of site surveys (e.g. Petrie *et al.*, 2022).

## Author statement

Utley: data curation (lead), formal analysis (lead), investigation (lead), visualization (lead), writing – original draft (lead), writing – review & editing (supporting).

Holdsworth: conceptualization (lead), funding acquisition (lead), investigation (supporting), project administration (lead), supervision (lead), writing – original draft (supporting), writing – review & editing (lead).

Walker: formal analysis (supporting), visualization (supporting), writing – review & editing (supporting).

Dempsey: investigation (supporting), supervision (supporting), writing – review & editing (supporting).

McCaffrey: supervision (supporting), formal analysis (supporting), writing – review & editing (supporting).

Dichiarante: conceptualization (lead), writing – review & editing (supporting).

Jones: data curation (supporting), formal analysis (supporting), investigation (supporting).

## Declaration of competing interest

The authors declare that they have no known competing financial interests or personal relationships that could have appeared to influence the work reported in this paper.

## Data availability

Data will be made available on request.

## Acknowledgements

The work contained in this paper was conducted during a PhD study undertaken as part of the Natural Environment Research Council (NERC) Centre for Doctoral Training (CDT) in Oil & Gas [grant number NEM00578X/1] and was funded by Durham University whose support is gratefully acknowledged. The BGS, UKHO and NSTA (previously OGA) are acknowledged for providing geological, bathymetric, and offshore data which is available and reproduced under OGL (Open Government Licence). Steve Andrews and an anonymous reviewer are thanks for their very constructive comments and reviews.

## Appendix A. Supplementary data

Supplementary data to this article can be found online at <https://doi.org/10.1016/j.jsg.2023.104922>.

## References

- Armitage, T.B., Watts, L.M., Holdsworth, R.E., Strachan, R.A., 2020. Late Carboniferous Dextral Transpressional Reactivation of the Crustal-Scale Walls Boundary Fault, Shetland: the Role of Pre-existing Structures and Lithological Heterogeneities. *Journal of the Geological Society, London*. <https://doi.org/10.1144/jgs2020-078>.
- Astin, T.R., 1985. The palaeogeography of the Middle Devonian lower Eday sandstone, Orkney. *Scot. J. Geol.* 21, 353–375. <https://doi.org/10.1144/sjg21030353>.
- Astin, T.R., 1990. The Devonian lacustrine sediments of Orkney, Scotland; implications for climate cyclicality, basin structure and maturation history. *J. Geol. Soc.* 147, 141–151. <https://doi.org/10.1144/gsjgs.147.1.0141>.
- Baxter, A.N., Mitchell, J.G., 1984. Camptonite-Monchiquite dyke swarms of Northern Scotland; Age relationships and their implications. *Scot. J. Geol.* 20, 297–308. <https://doi.org/10.1144/sjg20030297>.
- BGS, 1982. Caithness sheet 58 N - 04. *W Solid Geol.* 1, 250000 (Series).
- BGS, 1985a. Orkney sheet 59 N - 04. *W Solid Geol.* 1, 250000 (Series).
- BGS, 1985b. Thurso, Scotland sheet 116W. *Solid Ed.* 1 (50), 000.
- BGS, 1986. Wick, Scotland sheet 116E. *Solid Ed.* 1 (50), 000.
- BGS, 1999. Orkney Islands 1:100000 Special Provisional Map Solid and, Drift Edition.
- BGS, 2019. In: British Geological Survey Geindex Offshore. [mapapps2.bgs.ac.uk/geindex\\_offshore/home.html](http://mapapps2.bgs.ac.uk/geindex_offshore/home.html).
- Brown, J.F., Astin, T.R., Marshall, J.E.A., 2019. The Paleozoic petroleum system in the north of Scotland – outcrop analogues. In: Monaghan, A.A., Underhill, J.R., Hewett, A.J., Marshall, J.E.A. (Eds.), *Paleozoic Plays of NW Europe*, 471. Geological Society, London, Special Publications, pp. 253–280. <https://doi.org/10.1144/SP471.14>.
- Chapman, N.A., 1975. An experimental study of spinel clinopyroxene xenoliths from the Duncansby Ness vent, Caithness, Scotland. *Contrib. Mineral. Petrol.* 51, 223–230. <https://doi.org/10.1007/BF00372082>.

- Collier, J.S., Gupta, S., Potter, G., Palmer-Felgate, A., 2006. Using bathymetry to identify basin inversion structures on the English Channel shelf. *Geology* 34, 1001–1004. <https://doi.org/10.1130/G22714A.1>.
- Craven, B., Lloyd, G.E., 2023. Reconciling onshore and offshore geological mapping: lessons from N. Cornwall, SW England. In: *Geological Mapping – of Our World and Others*, 314. Geological Society of London, Special Publication (in press).
- Coward, M.P., Enfield, M.A., Fischer, M.W., 1989. Devonian basins of northern Scotland: extension and inversion related to late caledonian—variscan tectonics. *Geol. Soci., London, Spl. Pub.* 44, 275–308.
- Dichiarante, A.M., 2017. A Reappraisal and 3D Characterisation of Fracture Systems within the Devonian Orcadian Basin and its Underlying Basement: an Onshore Analogue for the Clair Group. Durham University. Unpublished PhD thesis.
- Dichiarante, A.M., Holdsworth, R.E., et al., 2016. New structural and Re–Os geochronological evidence constraining the age of faulting and associated mineralization in the Devonian Orcadian Basin, Scotland. *J. Geol. Soc.* 173, 457–473. <https://doi.org/10.1144/jgs2015-118>.
- Dichiarante, A.M., Holdsworth, R.E., Dempsey, E., McCaffrey, K.J.W., Utley, T.A.G., 2020a. The Outcrop-Scale Manifestations of Reactivation during Multiple Superimposed Rifting and Basin Inversion Events: the Devonian Orcadian Basin, N Scotland. *Journal of the Geological Society, London*. <https://doi.org/10.1144/jgs2020-089>.
- Dichiarante, A.M., McCaffrey, K.J.W., Holdsworth, R.E., Bjornarå, T.I., Dempsey, E.D., 2020b. Fracture attribute scaling and connectivity in the Devonian Orcadian Basin with implications for geologically equivalent sub-surface fractured reservoirs. *Solid Earth*. <https://doi.org/10.5194/se-2020-15>.
- Draper, S., Adcock, T.A.A., Borthwick, A.G.L., Houlsby, G.T., 2014. Estimate of the tidal stream power resource of the Pentland Firth. *Renew. Energy* 63, 650–657.
- Duncan, W.I., Buxton, N.W.K., 1995. New evidence for evaporitic Middle devonian lacustrine sediments with hydrocarbon source potential on the east Shetland platform, North Sea. *J. Geol. Soc.* 152, 251–258.
- Enfield, M.A., 1988. The Geometry of Normal Fault Systems and Basin Development: Northern Scotland and Southern France. Unpublished PhD thesis, Department of Geology, Imperial College.
- Enfield, M.A., Coward, M.P., 1987. The structure of the West Orkney Basin, northern Scotland. *J. Geol. Soc.* 144, 871–884. <https://doi.org/10.1144/gsjgs.144.6.0871>.
- Friend, P.F., Williams, B.P.J., Ford, M., Williams, E.A., 2000. Kinematics and dynamics of old red sandstone basins. In: Friend, P.F., Williams, B.P.J. (Eds.), *New Perspectives On the Old Red Sandstone*, 180. Geological Society, London, Special Publications, pp. 29–60.
- Hippler, S.J., 1989. Fault Rock Evolution and Fluid Flow in Sedimentary Basins. Unpublished PhD thesis, University of Leeds.
- Hippler, S.J., 1993. Deformation microstructures and diagenesis in sandstone adjacent to an extensional fault: implications for the flow and entrapment of hydrocarbons. *AAPG (Am. Assoc. Pet. Geol.) Bull.* 77, 625–637.
- Hodgetts, D., 2019. Virtual Reality Geological Studio. <https://www.vrgeoscience.com/>.
- Johnstone, G.S., Mykura, W., 1989. The northern highlands of Scotland. In: *British Regional Geology*, fourth ed. British Geological Survey, HMSO London.
- Macintyre, R.M., Cliff, R.A., Chapman, N.A., 1981. Geochronological evidence for phased volcanic activity in Fife and Caithness necks, Scotland. *Earth Environ. Sci. Transact. Royal Soci. Edinburgh* 72, 1–7.
- Marshall, J.E.A., Hewett, A.J., 2003. Devonian. In: Evans, D., Graham, C., Armour, A., Bathurst, P. (Eds.), *The Millennium Atlas: Petroleum Geology of the Central and Northern North Sea*. Geological Society of London, pp. 65–81.
- Martin-Short, R., Hill, J., Kramer, S.C., Avidis, A., Allison, P.A., Piggott, M.D., 2015. Tidal resource extraction in the Pentland Firth, UK: potential impacts on flow regime and sediment transport in the Inner Sound of Stroma. *Renew. Energy* 76, 596–607.
- Mauldon, M., Dunne, W.M., Rohrbaugh Jr., M.B., 2001. Circular scanlines and circular windows: new tools for characterizing the geometry of fracture traces. *J. Struct. Geol.* 23, 247–258.
- Mykura, W., Flinn, D., May, F., 1976a. *British Regional Geology: Orkney And Shetland*. HMSO, Edinburgh.
- Mykura, W., Pheister, J., Sabine, P.A., 1976b. The Geology of Western Shetland: Explanation of One-Inch Geological Sheet Western Shetland, Comprising Sheet 127 and Parts of 125, 126 and 128. *Memoirs of the Geological Survey of Great Britain (Scotland)*, HMSO, Edinburgh.
- Nixon, C.W., Sanderson, D.J., Bull, J.M., 2012. Analysis of a strike-slip fault network using high resolution multibeam bathymetry, offshore NW Devon U.K. *Tectonophysics* 541–543, 69–80. <https://doi.org/10.1016/j.tecto.2012.03.021>.
- Nyberg, B., Nixon, C.W., Sanderson, D.J., 2018. NetworkGT: a GIS tool for geometric and topological analysis of two-dimensional fracture networks. *Geosphere* 14, 1618–1634. <https://doi.org/10.1130/GES01595.1>.
- Oil and Gas Authority, 2019. Oil and Gas Authority Open Data. <http://data.ogauthority.opendata.arcgis.com/>.
- Ogilvie, S., Barr, D., Roylance, P., Dorling, M., 2015. Structural Geology and Well Planning in the Clair Field, 421. Geological Society, London, Special Publications, pp. 197–212. <https://doi.org/10.1144/SP421.7>.
- Petrie, H.E., Eide, C.H., Hafliadason, H., Watton, T., 2022. A conceptual geological model for offshore wind sites in former ice stream settings: the Utsira Nord site, North Sea. *J. Geol. Soc.* 179 <https://doi.org/10.1144/jgs2021-163>.
- Robertson, A.G., Ball, M., Costaschuk, J., Davidson, J., Guliyev, N., Kennedy, B., Leighton, C., Nash, T., Nicholson, H., 2020. 206/9a, 206/12a and 206/13a, UK atlantic margin. The Clair Field, Blocks 206/7a, 206/208. *Geol. Soci., London, Memoirs* 52 (1), 931. <https://doi.org/10.1144/petgeo2021-090>, 208.
- Rohrbaugh Jr., M.B., Dunne, W.M., Mauldon, M., 2002. Estimating fracture trace intensity, density, and mean length using circular scan lines and windows. *AAPG (Am. Assoc. Pet. Geol.) Bull.* 86, 2089–2104.
- Sanderson, D.J., Nixon, C.W., 2015. The use of topology in fracture network characterization. *J. Struct. Geol.* 72, 55–66. <https://doi.org/10.1016/j.jsg.2015.01.005>.
- Sanderson, D.J., Dix, J., Westhead, R.K., Collier, J.S., 2017. Bathymetric mapping of the coastal and offshore geology and structure of the Jurassic Coast, Weymouth Bay, UK. *J. Geol. Soc. London* 174. <https://doi.org/10.1144/jgs2016-070>.
- Seranne, M., 1992. Devonian extensional tectonics versus Carboniferous inversion in the northern Orcadian basin. *J. Geol. Soc.* 149, 27–37. <https://doi.org/10.1144/gsjgs.149.1.0027>.
- Shields, M.A., Dillon, L.J., Woolf, D.K., Ford, A.T., 2009. Strategic priorities for assessing ecological impacts of marine renewable energy devices in the Pentland Firth (Scotland, UK). *Mar. Pol.* 33, 635–642. <https://doi.org/10.1016/j.marpol.2008.12.013>.
- Tamas, A., Holdsworth, R.E., Underhill, J.R., Tamas, D.M., Dempsey, E.D., Hardman, K., Bird, A., McCarthy, D., McCaffrey, K.J.W., Selby, D., 2022a. New onshore insights into the role of structural inheritance during mesozoic opening of the inner Moray Firth Basin, Scotland. *J. Geol. Soc.* <https://doi.org/10.1144/jgs2021-066>.
- Tamas, A., Holdsworth, R.E., Underhill, J.R., Tamas, D.M., Dempsey, E.D., McCarthy, D., J., McCaffrey, K.J.W., Selby, D., 2022b. Correlating deformation events onshore and offshore in superimposed rift basins: the lossiemouth Fault Zone, inner Moray Firth Basin, Scotland. *Basin Res.* 00, 1–27. <https://doi.org/10.1111/bre.12661>.
- Tamas, A., Holdsworth, R.E., Tamas, D.M., Dempsey, E.D., Hardman, K., Bird, A., Underhill, J.R., McCarthy, D., McCaffrey, K.J., Selby, D., 2023a. Using UAV-based photogrammetry coupled with in situ fieldwork and U-Pb geochronology to decipher multi-phase deformation processes: a case study from sarcelt, inner Moray Firth Basin, UK. *Rem. Sens.* 15, 695. <https://doi.org/10.3390/rs15030695>.
- Tamas, A., Holdsworth, R.E., Tamas, D.M., Dempsey, E.D., Hardman, K., Bird, A., Roberts, N.M.V., Lee, J., Underhill, J.R., McCarthy, D., McCaffrey, K.J.W., Selby, D., 2023b. Older than you think: using U-Pb calcite geochronology to better constrain basin-bounding fault reactivation, Inner Moray Firth Basin, W North Sea. *J. Geol. Soc.* <https://doi.org/10.1144/jgs2022-166>.
- Trewin, N.H., 1993. *Geological History of East Sutherland and Caithness*. Excursion Guide to the Geology of East Sutherland and Caithness. Scottish Academic Press, Edinburgh.
- Westhead, K., Smith, K., Campbell, E., Colenutt, A., McVey, S., 2014. Pushing the boundaries: integration of multi-source digital elevation model data for seamless geological mapping of the UK's coastal zone. *Earth Environ. Sci. Transact. Royal Soci. Edinburgh* 105, 263–271.
- Wilson, R.W., Holdsworth, R.E., Wild, L.E., McCaffrey, K.J.W., England, R.W., Imber, J., Strachan, R.A., 2010. Basement-influenced rifting and basin development: a reappraisal of post-Caledonian faulting patterns from the North Coast Transfer Zone, Scotland. *Geol. Soci., London, Spl. Pub.* 335, 795–826. <https://doi.org/10.1144/SP335.32>.
- Witt, A.J., Fowler, S.R., Kjelstadli, R.M., Draper, L.F., Barr, D., McGarrity, J.P., 2010. Managing the start-up of a fractured oil reservoir: development of the Clair field, West of Shetland. *Petrol. Geol.: From Mat. Basins to New Front.—Proc. 7th Petrol. Geol. Conf.* 7, 299–313. <https://doi.org/10.1144/0070299>.
- Woodcock, N.H., Strachan, R.A. (Eds.), 2012. *Geological History of Britain and Ireland*, second ed. John Wiley & Sons.
- Yeomans, C.M., Head, M., Lindsay, J.J., 2021. Application of the tilt-derivative transform to bathymetric data for structural lineament mapping. *J. Struct. Geol.* <https://doi.org/10.1016/j.jsg.2021.104301>.